IMPROVED DESIGN OF A CLASS OF NETWORKED CONTROL SYSTEM

BY

YOUSIF A. AL-WAJIH

A Thesis Presented to the
DEANSHIP OF GRADUATE STUDIES

KING FAHD UNIVERSITY OF PETROLEUM & MINERALS

DHAHRAN, SAUDI ARABIA

In Partial Fulfillment of the
Requirements for the Degree of

MASTER OF SCIENCE

In

SYSTEM AND CONTROL ENGINEERING

MAY 2022

KING FAHD UNIVERSITY OF PETROLEUM & MINERALS
DHAHRAN 31261, SAUDI ARABIA

DEANSHIP OF GRADUATE STUDIES

This thesis, written by **YOUSIF A. AL-WAJIH** under the direction of his thesis adviser and approved by his thesis committee, has been presented to and accepted by the Dean of Graduate Studies, in partial fulfillment of the requirements for the degree of **MASTER OF SCIENCE IN SYSTEM AND CONTROL ENGINEERING**.

Thesis Committee

Dr. Nezar M. Al-Yazidi (Adviser)

Prof. Magdi S. Mahmoud (Member)

Dr. Mutaz M. Hamdan (Member)

Dr. Mujahed Aldhaefallah
Department Chairman

Dr. Suliman S. Al-Homidan
Dean of Graduate Studies

Date

To my parents and beloved wife
To those who care about me and whom I further care about

ACKNOWLEDGMENTS

All praise is to Almighty Allah and his beloved messenger Muhammad(SAWS). My grateful gratitude goes to King Fahd University of Petroleum and Minerals giving me the opportunity to complete my Masters Studies and providing me a great environment for education and research. I extend my deepest gratitude to my thesis advisor Dr. Nezar M. Al-Yazidi for his continuous support, patience and encouragement. He stood by me in all times and was the greatest support I had during my tenure in the university and most importantly during my thesis. I would also like to thank my thesis committee Prof. Magdi S. Mahmoud and Dr. Mutaz M. Hamdan for their time and valuable comments, especially Prof. Magdi who continuously supporting and encouraging me during my tenure in the university and during my thesis. I would also like to thank the Interdisciplinary Research Center for Smart Mobility and Logistics under project no. INML 2200. My heartfelt gratitude goes to my parents and beloved wife for their everlasting love, trust and faith in me. I could never have pursued my higher education without their encouragement and support. To my brothers, my sisters, grandfather, and uncles. Also I am thankful to all my family who have always loved and supported me in all forms of life, their love gives me immense strength to keep moving ahead. Last but not the least, I would like to thank all my friends and colleagues back at home and at KFUPM whose presence

and discussions were the biggest support during times of loneliness and despair. Things would not have been better if not for their continuous support, namely, Zead, Gubran, ...

TABLE OF CONTENTS

LIST OF TABLES

LIST OF FIGURES

THESIS ABSTRACT

NAME: Yousif A. Al-Wajih

TITLE OF STUDY: Improved Design of a Class of Networked Control System

MAJOR FIELD: System and Control Engineering

DATE OF DEGREE: May 2022

Sustaining the performance of the power grid at a desired operating point is a challenge in an uncertain environment. Multi-area interconnected power system is affected by the variation on the load due to the dynamic and the uncertainty of the environments. The variations on the load can negotiate the stability of the power systems. Due to the active load change and the dynamic environment and uncertainty a model-free controller is a suitable technique that can maintain reliable performance in this condition. The online adaptive policy control scheme is proposed for load frequency control (LFC) challenges in single and multi-areas power grids. The proposed scheme uses an optimal control approach through a modified Bellman equation and two neural networks one to approximate the proposed solving value function and the second one is to approximate the optimal control. Furthermore, With the continuous increase of the electricity demand, power systems are more essential for the modern lifestyle.

Recently, power generation areas have been connected to meet the demand load and provide customers with the required electricity such that if one generation area fails, others con cover the demand. Power systems are vulnerable to transmission delay and cyber-attacks which can affect the stability of the system and cause failure. In this work, we explore the stabilization of a multi-area interconnected power system (MAIPS) in the presence transmission Delay and denial of service (DoS) attack that prevents the exchange of data over the communication channel. First, a static feedback controller is designed to stabilize the MAIPS in the nominal situation. Then, the stability of the MAIPS is characterized when the system is subjected to the transmission Delay and the DoS attack while considering predetermined limits of the duration and the frequency of the delay. Finally, an illustrative example of three area interconnected power system with several scenarios are presented to verify the effectiveness of the proposed method, and the performance of the proposed model free adaptive control is compared with the model productive control.

ملخص الرسالة

الاسم: يوسف أحمد الوجيه

عنوان الرسالة: تصميم مطور لفئة من أنظمة التحكم الشبكيه

التخصص: هندسة نظم تحكم

تاريخ الدرجة العلمية: تاريخ الدرجة العلمية

يمثل الحفاظ على أداء مولدات الطاقة عند نقطة التشغيل المطلوبة تحديًا في بيئة غير مستقرةْ حيث أن نظام الطاقة المترابط متعدد المناطق يتأثر بالتغير في الحمل بسبب ديناميكية النظام و التغيرات و عدم أستقرار البيئات المثرة على النظام لذالك من الممكن أن تؤثر هذه الاختلافات في الحمل على استقرار أنظمة الطاقة المرتبظه بالشبكة. نظرًا لتغير الحمل النشط والبيئة الديناميكية ، فإن وحدة التحكم ضروريه للحفاظ على أداء موثوق في مثل هذه الحلات . لهذا السبب تم اقتراح متحكم يمكنه مواجهة هذه التحديات في شبكات الطاقة المفردة والمتعددة المناطق. يستخدم المتحكم المقترح نهج التحكم الأمثل من خلال معادلة رياضيةمعدلة وشبكتين عصبيتين واحدة لتقريب وظيفة قيمة الحل المقترحة والثانية لتقريب أشارة التحكم الأمثل. ومع الزيادة المستمرة في الطلب على الكهرباء ، أصبحت أنظمة الطاقة أكثر أهمية لنمط الحياة الحديث. في الآونة الأخيرة ، تم توصيل مناطق توليد الطاقة لتلبية حمل الطلب وتزويد العملاء بالكهرباء المطلوبة بحيث إذا تعطلت إحدى مناطق التوليد ، فإن مناطق أخرى تغطي الطلب. لهذا فإن أنظمة الطاقة عرضة لتأخير الإرسال والهجمات الإلكترونية التي يمكن أن تؤثر على استقرار النظام وتعطله. في هذا الرسالة ، تمت دراسة استقرار نظام طاقة مترابط متعدد المناطق في هجوم تأخير الإرسال ورفض الخدمة الذي يمنع تبادل البيانات عبر قناة الاتصال. أولاً ، تم تصميم وحدة التحكم في التغذية المرتدة الثابتة لتحقيق الاستقرار في الوضع الاسمي. بعد ذلك ، يتم تغيرعوامل الاستقرار عندما يتعرض النظام لتأخير الإرسال او هجوم مع مراعاة الحدود المحددة مسبقًا للمدة وتكرار التأخير. أخيرًا ، يتم تقديم مثال توضيحي لنظام طاقة مترابط من ثلاث مناطق مع عدة سيناريوهات للتحقق منها فعالية الطريقة المقترحة.

CHAPTER 1

INTRODUCTION

1.1 Background

With the extensive increase of economic and social development, the power industry plays an important role in our daily life. Meanwhile, the power grid operation is harshly degrading due to the dynamic deviation in the active load demand of interconnected generation areas. This challenge accelerates with propagating complexity of the interconnected power system by combining additional supplied generation areas into the presented power grids. Adding generation resources to the power system led to increase the probability of interconnected power system failures. The main reason for this issue is the diffusion of different frequency harmonics in the interconnected wide-area power grids [1]. Hence, the interconnected power system efficiency is violated due to dynamic alternatives in the active load demands [1], [2], [3], [4], [5]. In this content, the load frequency control (LFC) in the grid systems ultimately challenging and complex due to variations in the active load demands, modeling of the non-linear interconnected systems, and the uncertain environments dynamic [3]. In this manner,

a model-free control with the online adaptive policy iteration approach is developed to address a distributed LFC problem in the interconnected power grids. This work adopted the policy iteration procedures to solve the modified Bellman reported. As well, an adaptive critic method in real-time was used to estimate the distributed LFC signals for the interconnected area of power generation systems.

Recent advances in power systems have made an increase attention on the multi-area interconnected power system (MAIPS). To support control schematic in power systems, recent research was directed in applying different virtual inertia emulation methods to link the multi-power generations [6], [7], [8]. The control loops of load frequency control (LFC) communicate measurements and control data among the networks such as the supervisory control and data acquisition (SCADA) system. The standard control scheme of the LFC requires additional modifications to handle the new scenarios where power generation areas are interconnected. Therefore, a high dependence on data communication introduce time delay issues in the LFC since Interconnected power system, in this manner, has a high possibility to be affected by transmission delay that has the same affect as the Danial of Service attack [9], [10]. Furthermore, an intentional transmission delay on the LFC system could have an explicit effects on the system stability and frequency. In addition, it could cause severe damages to the economy of the interconnected power system [11]. In this circumstance, the transmission delay could eradicate the nominal operation of the interconnected system. On another word, the transmission delay could interrupt the dynamics of the system [12]. So, the stability analysis should be considered in the design of a MAIPS [13].

The LFC is a typical automatic closed-loop system in the MAIPS that keeps the interconnected system frequency stable in the typical situation. This objective is achieved by adjusting the set-points of area generators for active power output based on reserved measurement through the communication networks and wide-area transmitted measurements units [14]. However, the communication channels in wide-area measurements such as SCADA system could be affected by attackers, which means that LFC systems require more attention against cyberattacks [15].

Recent advances in power systems have made an increase attention on the multi-area interconnected power system (MAIPS). To support control schematic in power systems, recent research was directed in applying different virtual inertia emulation methods to link the multi-power generations [6], [7], [8].The control loops of load frequency control (LFC) communicate measurements and control data among the areas communication networks such as the supervisory control and data acquisition (SCADA) system. The standard control scheme of the LFC requires additional modifications to handle the new scenarios where power generation areas are interconnected. Therefore, a high dependence on data communication introduce security issues in the LFC since Interconnected power system, in this manner, has a high possibility to be affected by several cyber attacks without rising any notification before the failure [9], [10]. Furthermore, an intentional attack targeted the LFC system could have an explicit effects on the system stability and frequency. In addition, it could cause severe damages to the economy of the interconnected power system [11]. In this circumstance, an attacker may get an access to the supervision centers or the network channel in illegal way, then he could destroy the nominal operation of the intercon-

nected system. In another word, the attacker could interrupts the dynamics of the system. This lack of security protection either in hardware or software strategies give the attacker the ability to produce any perturbation [12]. So, the stability analysis should be considered in the design of a MAIPS.

1.2 Multi-area Interconnected Power System Model

A discrete-time MAIPS model linearized around operation points is considered in this brief. The MAIPS of thermal power station with single state turbines equipped with PI controller utilized. The mathematical model of the time-invariant MAIPS is represented in (1.1). Let N refer to a set of areas index, where the areas are connected through tie-lines. For this case, the subsystems are communicated thought the communication network, and the model that describes this is described as follows.

$$\begin{aligned} x_i(k+1) &= A_{ii}x_i(k) + B_i u_i(k) \\ &\quad + E_i f_i(k) + \sum_{j \in N} A_{ij} x_j(k) \\ y_i(k) &= C_i x_i(k) \end{aligned} \tag{1.1}$$

where for $x_i(k) = [\Delta\omega, \Delta P_{mech}, \Delta P_{vi}, \Delta P_{tie,i}]^T \in \Re^n$ denotes the states of the system frequency deviation, mechanical power deviation, steam valve position deviation, and deviation of the total tie-line power flow, respectively. $u_i \in \Re^m$ denotes the control signal of each subsystem. $f_i(k)$ is donating the load variation of i-th area. $y_i \in \Re^p$

denote the system observation, and f_i is defined as

$$f_i(k) = \begin{cases} \Delta P_{Li} & , k \leq \beta \\ 0 & , \beta \leq k \end{cases} \tag{1.2}$$

Where ΔP_{Li} is the local variation on the demeaned load that considered as a local disturbance in area i. β is a Bernoulli random variable with $P_l(k = 1) = 1 - p_l$ with load change probability p_l. . In [16] the model is discussed in detailed. Area Control Error (ACE) is an indication of the power mismatch between the generation and area load. The ACE expressed as a summation of frequency deviation and tie-line power change in any control area i. The illustrative diagram of MAIPS of single, and three subareas is shown in **Figure 1.1**, and **Figure 1.2**, respectively. The system matrices

defined as:

$$
\begin{aligned}
A_{ii}(N_{ij}) &= \begin{bmatrix} -\frac{D_i}{M_i^a} & \frac{1}{M_i^a} & 0 & -\frac{1}{M_i^a} \\ 0 & -\frac{1}{T_{CH_i}} & \frac{1}{T_{CH_i}} & \\ -\frac{1}{R_i^f T_{gi}} & 0 & -\frac{1}{T_{gi}} & 0 \\ \sum_{j\in N} T_{ij} & 0 & 0 & 0 \end{bmatrix} \\
B_i &= \begin{bmatrix} 0 \\ 0 \\ \frac{1}{T_{g_i}} \\ 0 \end{bmatrix}, \qquad E_i = \begin{bmatrix} -\frac{1}{M_i^a} \\ 0 \\ 0 \\ 0 \end{bmatrix} \\
A_{ij} &= \begin{bmatrix} 0 & 0 & 0 & 0 \\ 0 & 0 & 0 & 0 \\ 0 & 0 & 0 & 0 \\ \sum_{j\in N} T_{ij} & 0 & 0 & 0 \end{bmatrix} \\
C_i &= [1 \quad 0 \quad 0 \quad 1]
\end{aligned} \tag{1.3}
$$

In what follows, the multi-area system is represented by model (1.1). The target in this work is to design an appropriate control algorithm using adaptive policy iteration to ensure the close loop stability of power system under the load variation. The proposed algorithm has the ability to return the frequency of the power plant to the desired operating point even if the load changes. In this manner, The controller will ensure the stability of the MAIPS by utilizing the data of the subsystem and its connected neighbors to compute the input control signals for each time step.

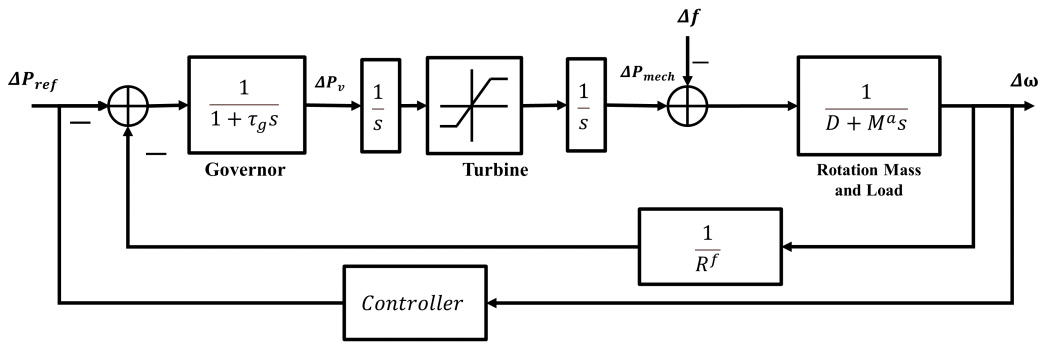

Figure 1.1: Block diagram of an isolated power system.

The generated policy aim, at guaranteeing the stability of the single and multi-area power network systems connected by the tie lines. We will configure the online adaptive policy iteration as a second-level control structure. The first controller in this system is the PI controller which works fine in the case of a single-area system but in the case of two connected areas and multi-area, such controller will fill down [17]. The idea of a two-level control structure is to let a local controller deal with the local dynamic and the structure of each subsystem while the global controller is aiming to compensate for the group behavior and performance.

1.3 Survey of Existing Literature

1.3.1 Output Control with Time delay and DoS attack

The communication among the generation areas in the MAIPS occurred in a common network medium. This grid required to be protected against the vulnerability of

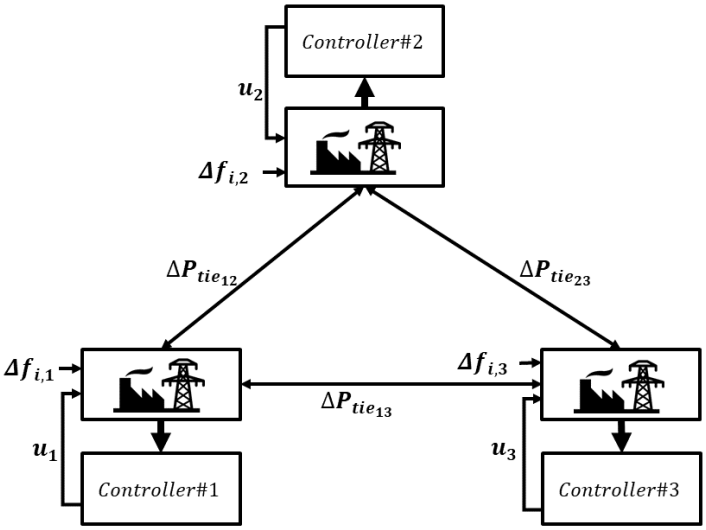

Figure 1.2: Diagram of MAIPS For $N = 3$.

attacks during the transmission of the data. As mentioned before, the system could be derived to volatility, or it may cause redundancy in the operation of the plant. Consequently, reflecting security subjects is very essential in the controllers' design for the MAIPS [18], [19]

Recent research activities are considering the impact of the transmission delay on conventional LFC systems with AC transmission lines. very few research were studied the effect of the transmission delay on the power network systems [20], [20]. The micro-grid LFC system with constant communication delays was presented in [21], where delay margins concerning PI gains are obtained. in [13], authors studied a decentralized LFC strategy based on switching control theory with presenting a transmission delay on the subsystem, while in [22] the problem of the load frequency

Table 1.1: Generation areas parameters

Symbol	Definition
ω	Angular rotating mass frequency
M_i^a	Angular momentum of $i-th$ subsystem
P_{mech}	Mechanical power
P_v	Steam valve position
T_{ch}	Prime mover charging time constant
f_i	Non-frequency-sensitive load change deviation
R^f	Percent Change in frequency divided by percent change in unit output
D_i	Change in percentage of (load/change in frequency).
T_g	Time constant of governor.
T_{ij}	Slope of the power angle curve at the initial operating angle between area i and area j.
T_{tie}^{ij}	Power flow of the tie-line between area i and area j
$T_{tie,i}$	Total power flow of the tie-line between area i and area j

control with presence of constant and the power system time-varying delays in state and control input was investigated.

Recently, researchers widely used the small gain approached to solve the stabilization problem of distributed systems. To maintain the stability of large-scale systems in the presence of a limited communication medium, an event-triggered sampling scheme was examined with distributed controllers in [23]. Also, the initial state is assured to be restored for a complex system in the case of mixed attacks in independent transmitting channels, Song et al. proposed a robust pinning synchronization control problem [24]. A hierarchical game method was presented in [25] for solving the control challenge of a wireless networked control system affected by DoS attack.

The LFC is a typical automatic closed-loop system in the MAIPS that keeps the interconnected system frequency stable in the typical situation. This objective is achieved by adjusting the set-points of area generators for active power output based on reserved measurement through the communication networks and wide-area transmitted measurements units [14]. However, the communication channels in wide-area measurements such as SCADA system could be affected by attackers, which means that LFC systems require more attention against cyber attacks [15].

The communication among the generation areas in the MAIPS occurred in a common network medium. This grid required to be protected against the vulnerability of attacks during the transmission of the data. As mentioned before, the system could be derived to volatility or it may cause redundancy in the operation of the plant. Consequently, reflecting security subjects is very essential in the controllers' design for the MAIPS [18],[19].

More frequently attacks strategies implemented are the DoS attacks where the attacker aims to occupy the communication channel to prevent the transmission of measurements or control signals thus cause a maximum failing of the performance of the system. Several control systems influenced by DoS attacks were discussed in the literature since they they could have high consequence [18].

Recent research activities are considering the impact of the attacks on conventional LFC systems with AC transmission lines. In [26], influences of data integrity attacks on the stability of the LFC are presented. For data availability attacks on LFC loops, there are some studies start exploring the effects of such kinds of attacks on LFC loops. Liu, S. et al. [27], illustrate the effect of DoS attacks on the LFC system

and its dynamics. It has been shown that the LFC system is unstable under DoS attacks. Rahimi, K. et [28] emphases the effect of time-delay attacks on the system dynamics of a multi-area LFC, proving that in the area where there is a change in the load, an availability attack could be more hazardous. a linear discrete-time model that includes the effects of different communication delays in the LFC model is intended to discover the stability issues on the power system [29]. Similar studies on communication delay/packet loss in conventional LFC models of normal AC systems can be found in [30], [31], [32].

1.3.2 Adaptive and Model productive Control

The classical integral LFC approaches were impeded in the power system yielding, balances the overshoot, the desired raising time, and desired to characteristics in the response of the power areas generations [33], [1]. An adaptive proportional-integral (PI) method was addressed for load frequency regulation in [34]. This arrangement fulfilled the hyper-stability condition in the uncertainty of the dynamic environment. A μ-synthesis method for the robust LFC was examined in [35]. An approach that combined the matching condition with Lyapunov stability theory was tested on an LFC design [36]. A design of an automatic generation control (AGC) was proposed with assets of a closed-loop method based on the pole-placement techniques [37]. A design of a PI- LFC approach using a fuzzy gain scheduling technique was reported in [38], [39]. This method exhibited better characteristics than the fixed-gain control approach. An approach of decentralized LFC scheme based on diagonal dominance is tested in the [40]. In this manner, where the LFC system can be designed inde-

pendently while a singular value structure can be satisfied. In [33], a two degree of freedom regulation model based on the proportional integral derivative (PID) control is present.

The linear matrix inequality (LMI) approach was employed for building a robust decentralized LFC in [41], while another LMI scheme was deployed in interconnected power systems with implementing a delay in the communication in [42]. In [43] authors proposed a power angel derivative controller based on measurement error filtering and left-difference estimation to tackle the synchronization problem of the multi-machine power system under measurement errors,parameter uncertainties, and emergency modes. In [44] a model productive control (MPC) scheme was used to design for LFC in a single area of power system with the wind turbine, however a review of MPC in microgrids was carried in [45]. In [5], distributed-MPC is proposed for a multi-areas power system with a guarantee of stability while a tube-based MPC was proposed in [46] to provide efficient control signals for improving the response of the aggregated Electric Vehicles for Frequency Regulation of an Isolated Power Grid. In [47] an adaptive power control strategy based on sliding mode control is presented for the operation of islands microgrids.

In [48] AGC gain scheduling is implemented with a recursive least square approach combined with a genetic algorithm and fuzzy system both utilized to estimate the power system parameters in real-time. In [49], [50], a two level control approach was used for an interconnected power system. The primary level of control is implemented to control the local power unit while the secondary level controller was designed to coordinate the interconnected units. In [51]. LFC approach based on

automated learning which can extend and classify power grid was presented. Using the bio-geography-based optimization technique to select the gain for the integral-derivative (ID) FLC was presented in [52]. A decentralized LFC using a sliding mode technique is proposed in [53] for interconnected power systems with delay. To overcome the communication delay between the areas of power generations a dynamic control method is examined in [54]. The performance exhibits a limitation because of the bandwidth of the controller.

Some approximation methods are used to unravel the optimal control issues. These categories are diverse from one solution to another and they can tackle complex problems since most of them are associated with dynamic programming [55], [56], [57]. In this manner, the control problem is involving an optimization process where the cost function aim is to generate sequentially different control signals. The Bellman optimality equation is formulated to assist the optimal control methods in [58], [59]. The reinforcement learning (RL) techniques with approximate dynamic programming were utilized in solving the optimal control challenges with help of adaptive critic and actor neural network [55], [56], [57], [60]. To reduce the cumulative error of the cost function of the formulated optimality problem the RL is adapted to provide a dynamic solution platform for the control problem [57], [61]. To sum up, two main steps are implemented in this control method. The first step in solving the difference system equation by approximating means, followed step is to select the optimal control policy using actor-network [57], [61], [62]. A comprehensive literature on the intelligent and adaptive techniques that have been applied to microgrids systems was discussed in [63]. A single-machine infinite-bus system with a static variable controller is described

in [64] and its transient stability issue is solved using adaptive back stepping control, an improved back stepping method, and sliding mode variable structure control.

1.4 Problem Statement

The most common challenge on the networked control systems is the time delay and the packet dropout of the communication signals. In this manner, the time delay and packet dropout must be presented on control systems design to guarantee the stability of the close loop system. Multi-area Interconnected Power System is considered as a class of large scale NCS that can be used to test the proposed control techniques.

1.5 Objectives of the Thesis

The prime target of this study is to design a controller for a class of networked control system. Where the following are the specific objectives of this study:

- To cast the model of the networked control system (NCS) in a framework that can accommodate time delay, packet dropout, communication constraints.
- To examine the effect of system interconnection and the time delay on the dynamic system and the stability of the system.
- Finally, designing an improved approach to ensure the stability of NCS by utilizing the recent control techniques.

Therefore, the proposed method to achieve the objective of the proposed work is given as following main stages:

- Carrying on a comprehensive literature review on networked control systems.
- Exploring the system proposed in literature by reflecting and reproducing some of the results to understand the model and extending this approach by adding constraints on the networked system.
- Analyzing the networked control system and designing a control technique for the system.
- Simulating the results using simulation platforms such as MatLab.

1.6 Thesis Structure

The remaining of the thesis is composed of five chapters. In chapter 1.3 a survey of the existing control techniques is carried. Chapter 2 a stability analysis base on an output feedback controller is proposed to stabilize a MAIPS when the system is under transmission delay. where in chapter 3 a stability analysis is carried to stabilize a MAIPS when the system is subject to Danial of Service (DoS) attack. In chapter 4 an adaptive controller with policy iteration is proposed and it performance is compered with the model productive control techniques. The conclusion and the future work is discussed in chapter 5.

CHAPTER 2

STABILITY ANALYSIS UNDER TRANSMISSION DELAY

2.1 Introduction

More practical implementation in the real systems is the transmission Delay where the communication channel are pausing the transmission of measurements or control signals thus cause a maximum failing of the performance of the system. Several control systems influenced by transmission delay including MAIPSs. MAIPSs are representative examples of networked control systems, where control loops are closed using a communication channel. As in any large-scale system, time delays occurring during transmission become critical since time delays in LFC systems may destabilize the closed-loop system and degrade dynamic performance [18][65].

The challenge in this subject is to design an output feedback controller and a method with a parameter based on the output signals that guarantee the stability of a MAIPS subject load deviation and a transmission delay. The contribution of this

article can be summarized as follows:

- We design an output feedback controller to stabilize a MAIPS with load deviation when the system is under transmission delay.
- The limits on the frequency and duration of the transmission delay are characterized for a MAIPS that implements a typical Round robin communication protocol.
- The stability of a discrete time MAIPS is discussed and analyzed such that the stability is maintained in the presence of transmission delay and load change.
- An illustrative example of a typical MAIPS is provided with several scenarios considering the designed controller with the typical and the modified sampling time in the absent and presence of a transmission delay to verify the effectiveness of the proposed approach and controller.

Considering the MAIPS described by model (1.1). The target is to design an appropriate feedback controller to guarantee the close loop stability of all areas on the power network. N in the model is representing the set of the neighbor's agent j. In this manner, the controller proposes to use the output feedback measurements of the subsystems to compute the input control signals for each time step as a distributed system. The controller goal is to ensure the stability of the MAIPS. The diagram of the system with three areas was shown in **Figure 2.1**.

The remaining of the chapter is organized as follows: The modeling of a MAIPS is presented in Section 1.2. In Section 2.2, the framework is provided. Then, the

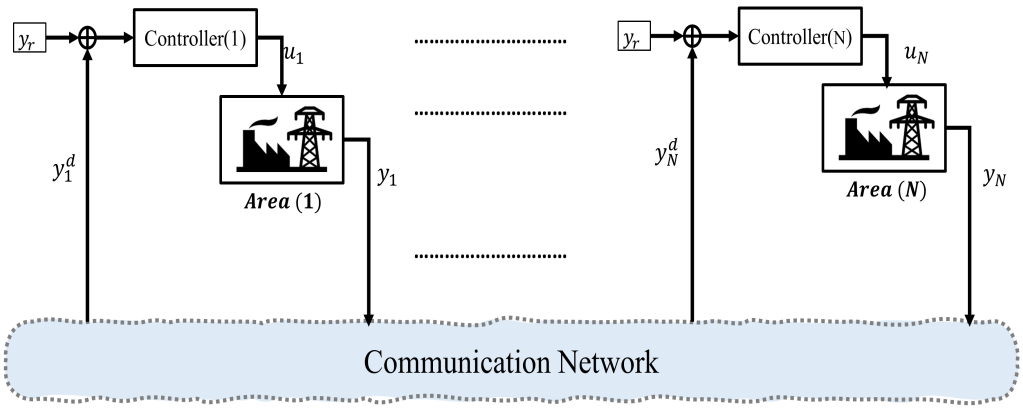

Figure 2.1: Scheme of MAIPS with Communication Channel

output feedback controller and stability analysis of a MAIPS is discussed in Section 2.3. Finally the simulation of an illustrative example is presented in Section 2.4.

2.2 Framework

Let's consider the discrete MAIPS expressed in Section 1.2. In (1.1) is the mathematical model of $i-th$ subsystem on MAIPS. A communication network is used to transfer the data and measurements as shown in **Figure 2.1**. A feedback controller use the measurements to figure the control signals and forward them to the actuators of the systems to maintain a certain frequency of the grid at the desired frequency. In ideal situation, the signals arrive to the control unit with no time delay in a sample-and-hold manner. For example, $y_i(k_i^r)$ where k_i^r refer to the received communication

attempts.

Remark 1 *We assume the output feedback gains K_i and L_{ij} are existed that press all eigenvalues of matrix $\bar{A}_i$ to have norm strictly less than one, i.e. each feedback area is Schur stable.*

2.2.1 Transmission Delay

In this section, the time delay is induced in the multi-area interconnected power system. To present the time delay on the MAIPS, let's consider the sampling time T_s with a constant sampling period $T_s = t_{k+1} - t_k$ and stochastic time delay d_k. The sampling period at the controller is rewritten as in assumption (1).

Assumption 1 *Let h is the fixed ideal period of sampling and the delay d_k is random and limited to $d_k < d_{max}$.*

$$T_s \quad = \quad h + d_k \tag{2.1}$$

where d_k and h_k are restricted to this condition $0 < d_k < h_k$ and $0 < h_{min} < h_k < h_{max}$. However, d_k is independent and has a known distribution with an occurring frequency f_k.

Assumption 2 *Let the constants $\lambda \in \mathbb{N}, \theta \in \mathbb{N}$ and d_{max} and f_{max} exist such that*

time delay $d_k \in [\tau, k]$ *and* f_{max} *have the following constraints :*

$$\begin{aligned} \mid d_k \mid &\leq \lambda + d_{max}(k-\tau) && (2.2) \\ f_d &\leq \theta + \frac{(k-\tau)}{f_{max}} && (2.3) \end{aligned}$$

Where $k \geq \tau$ *for all* k *and* τ*.*

We remark that the communication network generated a time delay d_k that is less than h_k but the packets correctly received. By considering discrete-time dynamic (1.1) with measurements delay d_k. The subsystem dynamic is written as:

$$y_i^d(k) = \begin{cases} C_i x_i(k-d_k) & ,\gamma(k)=1 \\ C_i x_i(k) & ,\gamma(k)=0 \end{cases} \quad (2.4)$$

Where $\gamma(k)$ is a Bernoulli random variable with $P_r(k=1) = p_k$. y_i^d refer to received measurements of $i-th$ area. So, the system in (1.1) is rewritten as

$$\begin{aligned} x_i(k+1) &= A_{ii}x_i(k) + B_i u_i(k) + E_i f_i(k) + \sum_{j \in N} A_{ij} x_j(k) && (2.5) \\ y_i^d(k) &= \gamma C_i x_i(k) + (1-\gamma) C_i x_i(k-d_k) \end{aligned}$$

Remark 2 *Each control input* u_i *affecting subsystem* i *consists of two parts. The first part depends on the area output with a gain of* K_i*, second one is depends on the area neighbors' output with a gain of* L_{ij}*, such control signal is given by:*

$$u_i(k) = K_i y_i^d(k) + \sum_{j \in N_i} L_{ij} y_i^d(k) \quad (2.6)$$

Where K_i and L_{ij} denote the controller gains.

2.3 Output Feedback Controller and Stability Analysis

The aim is to administrate the stability of the MAIPS in the normal situation or with the presence of the communication time delay. Mainly we address the stabilization problem of MAIPS connected by tie-line in the nominal situation and under the influence of transmission delay.

At each transmission instant, let $e_i(k)$ refer to the error between the received states $x_i^d(k)$ and the actual states $x_i(k)$ in each i-area. So, it could be written as:

$$e_i(k) = x_i^d(k) - x_i(k), \quad i = 1, 2, \ldots, N \tag{2.7}$$

The objective of this work is to design an output feedback controller as in (2.6) that guarantee the stability of the close loop model described in (1.1). On the coming section, the Lyapunov theory is used to ensure the system (1.1) is exponentially stable.

The $i-th$ subsystem dynamic could be rewritten by substituting (2.7), and (2.6) in (1.1), such as

$$\begin{aligned} x_i(k+1) &= A_{ii}^c x_i(k) + B_i K_i C_i e_i(k) + E_i f_i(k) + \sum_{j \in N} A_{ij}^c x_j(k) + \sum_{j \in N} B_i L_{ij} C_j e_j(k) \\ A_{ii}^c &= A_i i + B_i K_i C_i, \quad A_{ij}^c = A_i j + B_i L_{ij} C_j \end{aligned} \tag{2.8}$$

From close loop system (2.8), It could be noted that $i-th$ area is effected by the $f_i(k)$ in additional to $x_j(k)$, $e_i(k)$, and $e_j(k)$ the interconnected neighbors and errors, respectively.

Remark 3 *As illustrated in (2.8) the stability can be achieved in a weak couplings situation and within a small error e. Besides, a design parameter σ has been introduced to clarify the "smallness" of e.*

Assumption 3 *(Inter-sampling interval). With nonexistence transmission delay there is an inter-sampling interval (Δ) satisfying:*

$$\|e_i(k)\| \leq \sigma_i \|x_i(k)\| \tag{2.9}$$

σ_i here is holds as a design factor. According to [66], the selection and design of Δ and σ_i is essential to guarantee the stability of the distributed systems.

Remark 4 *Even if Δ is not shown explicitly in (2.9), it can be noticed from the definition of the error (2.7) that the inter-sampling interval affect the stability of the system. Referring to Remark 3, Assumption 3 guarantees the "smallness" of the error by selecting a proper inter-sampling interval.*

Remark 5 *It is worth to mention that the designing of the inter-sampling interval, Δ in (2.9) is a considerable problem. An inter-sampling interval satisfying limits as (2.9) could be precisely resolved for centralized settings [66]. While some literature computes and applies a lower bound of time elapsed between two events to avoid Zeno behavior in asymptotically stable distributed/decentralized systems [67], [68].*

2.3.1 Static output feedback control design

In this section, the main objective is to design a static output feedback controller in the form of (2.6) to achieve the asymptotic stability for nominal distributed systems (1.1).

For static output feedback control design, the following two theorems are established.

Theorem 2.1 *If the controller gains K_i and L_{ij} in (2.6) is given. The system in (1.1) is asymptotically stable if positive matrices P_i exist and satisfying the following:*

$$\Xi_i = \begin{bmatrix} \Xi_{1i} & \Xi_{2i} & \Xi_{3i} & \Xi_{4i} & \Xi_{5i} \\ * & \Xi_{6i} & \Xi_{7i} & \Xi_{8i} & \Xi_{9i} \\ * & * & \Xi_{10i} & \Xi_{11i} & \Xi_{12i} \\ * & * & * & \Xi_{13i} & \Xi_{14i} \\ * & * & * & * & \Xi_{15i} \end{bmatrix} < 0 \tag{2.10}$$

Where

$$\begin{aligned}
\Xi_{1i} &= A_i^{cT} P_i A_i^{cT} - P_i, \quad \Xi_{2i} = 2A_i^{cT} P_i B_i K_i C_i; \qquad (2.11)\\
\Xi_{3i} &= 2A_i^{cT} P_i E_i, \quad \Xi_{4i} = 2A_i^{cT} P_i \sum_{j\in N} A_{ij}^c,\\
\Xi_{5i} &= 2A_i^{cT} P_i \sum_{j\in N} B_i L_{ij} C_j, \quad \Xi_{6i} = C_i^T K_i^T B_i^T P_i B_i K_i C_i,\\
\Xi_{7i} &= 2C_i^T K_i^T B_i^T P_i E_i, \quad \Xi_{8i} = 2C_i^T K_i^T B_i^T P_i \sum_{j\in N} A_{ij}^c,\\
\Xi_{9i} &= 2C_i^T K_i^T B_i^T P_i \sum_{j\in N} B_i L_{ij} C_j, \quad \Xi_{10i} = E_i^T P_i E_i\\
\Xi_{11i} &= E_i^T P_i \sum_{j\in N} A_{ij}^c, \quad \Xi_{12i} = E_i^T P_i \sum_{j\in N} B_i L_{ij} C_j\\
\Xi_{13i} &= \sum_{j\in N} A_{ij}^{cT} P_i A_{ij} A_{ij}^c, \quad \Xi_{14i} = \sum_{j\in N} A_{ij}^{cT} P_i B_i L_{ij} C_i\\
\Xi_{15i} &= \sum_{j\in N} C_j^T L_{ij}^T B_i^T P_i B_i L_{ij} C_j
\end{aligned}$$

Proof. To proof theorem 2.1, the following Lyapunov function is considered.

$$V_i(k) = x_i^T(k) P_i x_i(k) \qquad (2.12)$$

Now, by evaluating $\Delta V_i(k))$ as follows:

$$
\begin{aligned}
\Delta V_i(k) &= V_i(k+1) - V_i(k) \\
\Delta V_i(k) &= x_i^T(k)(A_i^{cT} P_i A_i^{cT} - P_i)x_i(k) + 2x_i^T(k)A_i^{cT} P_i B_i K_i C_i e_i(k) \\
&\quad +2x_i^T(k)A_i^{cT} P_i E_i f_i(k) + 2x_i^T(k)A_i^{cT} P_i \sum_{j\in N} A_{ij}^{cT} x_j(k) \\
&\quad +2x_i^T(k)A_i^{cT} P_i \sum_{j\in N} B_i L_{ij} C_j e_j(k) + e_i^T(k)C_i^T K_i^T B_i^T P_i B_i K_i C_i e_i(k) \\
&\quad +2e_i^T(k)C_i^T K_i^T B_i^T P_i E_i f_i(k) + 2e_i^T(k)C_i^T K_i^T B_i^T P_i \sum_{j\in N} A_{ij}^{cT} x_j(k) \\
&\quad +2e_i^T(k)C_i^T K_i^T B_i^T P_i \sum_{j\in N} B_i L_{ij} C_j e_j(k) + f_i^T(k)E_i^T P_i E_i f_i(k) \\
&\quad +2f_i^T(k)E_i^T P_i \sum_{j\in N} A_{ij}^{cT} x_j(k) + 2f_i^T(k)E_i^T P_i \sum_{j\in N} B_i L_{ij} C_j e_j(k) \\
&\quad + \sum_{j\in N} x_j^T(k)A_{ij}^{cT} P_i A_{ij} x_j(k) + 2\sum_{j\in N} x_j^T(k)A_{ij}^{cT} P_i B_i L_{ij} C_i e_j(k) \\
&\quad + \sum_{j\in N} e_j^T(k)C_j^T L_{ij}^T B_i^T P_i B_i L_{ij} C_j e_j(k) \qquad (2.13)
\end{aligned}
$$

To rewrite the aforementioned in the compact form let.

$$
\Theta_i^T(k) = \begin{bmatrix} x_i(k) & e_i(k) & f_i(k) & \sum_{j\in N} x_j(k) & \sum_{j\in N} e_j(k) \end{bmatrix}^T \qquad (2.14)
$$

then

$$
\Delta V_i(k) = \Theta_i^T(k)\Xi_i\Theta_i(k) \qquad (2.15)
$$

and Ξ_i as characterized in (2.10). ∎

Theorem 2.2 *If there exist positive definite matrices X_i, Y_i, Y_{ij}, M_i, R_i, M_{ij}, R_{ij},*

and positive scalars ϵ_i such that the following bilinear matrix inequality (BMI) is satisfied

$$\bar{\Xi}_i = \begin{bmatrix} -X_i & 0 & 0 & 0 & 0 & Y_i^T B_i^T + X_i A_{ii}^T \\ 0 & -\epsilon_i I & 0 & 0 & 0 & Y_i^T B_i^T \\ 0 & 0 & -\epsilon_i I & 0 & 0 & X_i E_i^T \\ 0 & 0 & 0 & -\epsilon_i I & 0 & \sum_{j\in N} Y_j^T B_i^T + X_i A_{ij}^T \\ 0 & 0 & 0 & 0 & -\epsilon_i I & \sum_{j\in N} Y_j^T B_i^T \\ * & * & * & * & * & -X_i \end{bmatrix} < 0$$
$$M_i C_i = C_i X_i, \qquad M_{ij} C_j = C_j X_i \tag{2.16}$$

Then, the system (2.8) is asymptotic stable with the designed observer controller in (2.6) where K_i, and L_{ij} are given as:

$$K_i = R_i M_i^{-1}, \quad L_{ij} = R_{ij} M_{ij}^{-1} \tag{2.17}$$

Proof. Ξ_i in LMI (2.10) can be rewritten as:

$$\Xi_i = \bar{\Xi}_{i11} + \bar{\Xi}_{i12} P_i \bar{\Xi}_{i12}^T < 0 \tag{2.18}$$

with $\bar{\Xi}_{i11} = \text{diag}\{-P_i, 0, 0, 0, 0\}$ and $\bar{\Xi}_{i12}^T = \begin{bmatrix} A_i^c & B_i K_i C_i & E_i & \sum_{j\in N} A_{ij}^c & \sum_{j\in N} B_i L_{ij} C_j \end{bmatrix}^T$. So, (2.18) is formulated using

Schur complements as:

$$\begin{bmatrix} \bar{\Xi}_{i11} & \bar{\Xi}_{i12} \\ \bar{\Xi}_{i12}^T & -P_i^{-1} \end{bmatrix} < 0 \tag{2.19}$$

Now, let $X_i = P_i^{-1}$, and multiply (2.19) from left and right by $\text{diag}\{X_i, X_i, X_i, X_i, X_i, I\}$. Recalling of the values of A_i^c, and A_{ij}^c and selecting $M_i\bar{C}_i := \bar{C}_i X_i$, $R_i := K_i M_i$, $Y_i := R_i C_i$, $M_{ij}C_j := C_j X_i$, $R_{ij} := L_{ij}M_{ij}$, and $Y_{ij} := R_{ij}C_j$, the BMI can be obtained as in (2.16). ∎

Remark 6 *Theorem 2.2 was established in view of the work presented by Mahmoud and Nounou in [69].*

2.3.2 A small-gain approach for a MAIPS

By choosing the Lyapunov function $V_i(k) = x_i^T(k)P_i x_i(k)$ where $Q_i = Q_i^T > 0$, and P_i is the unique solution of the Lyapunov equation $\bar{A}_i^T P_i \bar{A}_i - P_i + Q_i = 0$. Then each subsystem i should satisfy:

$$\lambda_{\min}(P_i)\|x_i(k)\|^2 \leq V_i(x_i(k)) \leq \lambda_{\max}(P_i)\|x_i(k)\|^2 \tag{2.20}$$

thus $\lambda_{\min}(P_i)$ is the smallest eigenvalue of of P_i and $\lambda_{\max}(P_i)$ is the largest. To maintain the stability of the system, σ_i must be selected base on lemma (2.1).

Lemma 2.1 *For MAIPS described by (1.1) that controlled by (2.6). Let $\mu \in \mathbb{R}^{N^+}$ to*

be any column vector satisfy $\mu^T A < 0$. *Then, the MAIPS is asymptotically stable if there is* $\sigma_i \forall i \in N$ *such that*

$$\sigma_i < \sqrt{\frac{l_i}{j_i}} \tag{2.21}$$

Where for l_i *refers to the* i*-th vector of* $L := \mu^T(-A + \bar{\Psi})$*and* j_i *refers to the* j*-th vector* $J := \mu^T \Gamma$. *The matrices* A, Γ *and* Ψ *are defined below.*

Proof.

The Lyapunov function is formed in order to establish the main theorem is

$$V_i(k) = x_i^T(k) P_i x_i(k) \tag{2.22}$$

Now, let evaluate (ΔVi) as (2.13).Hence, the compact form is given in (2.15), and the difference equation (2.13) could be described by taken the norm as following:

$$\begin{aligned}
\Delta V_i(k) \;=\; & -\lambda(Q_i)\left\|x_i(k)\right\|^2 + \left\|2\bar{A}_i^T P_i B_i K_i C_i\right\| \left\|x_i^T(k)\right\| \left\|e_i(k)\right\| \\
& + \left\|2\bar{A}_i^T P_i \sum_{j\in N} B_i L_{ij} C_j\right\| \left\|x_i^T(k)\right\| \left\|e_i(k)\right\| + \left\|2\bar{A}_i^T P_i E_i\right\| \left\|x_i^T(k)\right\| \left\|f_i\right\| \\
& + \left\|2\bar{A}_i^T P_i \sum_{j\in N} \bar{A}_j\right\| \left\|x_i^T(k)\right\| \left\|x_j(k)\right\| + \left\|C_i^T K_i^T B_i^T P_i B_i K_i C_i\right\| \left\|e_i(k)\right\|^2 \\
& + \left\|2C_i^T K_i^T B_i^T P_i \sum_{j\in N} B_i L_{ij} C_j\right\| \left\|e_i^T(k)\right\| \left\|e_i(k)\right\| + \left\|2C_i^T K_i^T B_i^T P_i E_i\right\| \left\|e_i^T(k)\right\| \left\|f_i\right\| \\
& + \left\|2K_i^T C_i B_i^T P_i \sum_{j\in N} \bar{A}_j\right\| \left\|e_i^T(k)\right\| \left\|x_j(k)\right\| + \left\|\sum_{j\in N}(k) L_{ij} C_j B_i^T P_i B_i L_{ij}\right\| \left\|e_j^T\right\| \left\|e_j(k)\right\|
\end{aligned}$$

$$
\begin{aligned}
&+ \left\| 2 \sum_{j \in N} L_{ij} C_j B_i^T P_i E_i \right\| \|f_i\|^2 + \left\| 2 \sum_{j \in N} L_{ij} C_j B_i^T P_i \bar{A}_j \right\| \left\| e_j^T(k) \right\| \|x_j(k)\| \\
&+ \left\| E_i^T P_i E_i \right\| \|f_i\|^2 + \left\| 2 E_i^T P_i \sum_{j \in N} \bar{A}_j \right\| \left\| {f_i}^T \right\| \|x_j(k)\| \\
&+ \left\| \sum_{j \in N} {\bar{A}_j}^T P_i \bar{A}_j \right\| \|x_j(k)\|^2
\end{aligned} \tag{2.23}
$$

By utilizing Young's inequalities, assuming Z, V, and J any matrices with $\delta > 0$ consequently

$$
\|Z\| \|V\| \|J\| \leq \delta \|V\|^2 + \frac{1}{\delta} \|Z\|^2 \|J\|^2 \tag{2.24}
$$

By utilizing the inequalities (2.24) on (2.24) lead to:

$$
\begin{aligned}
\Delta V_i(x_i(k)) \leq & -\alpha_{ii} \|x_i(k)\|^2 + \psi \|f_i\| + \sum_{j \in N_i} \alpha_{ij} \|x_j(k)\|^2 \\
& + \gamma_{ii} \|e_i(k)\|^2 + \sum_{j \in N_i} \gamma_{ij} \|e_j(k)\|^2
\end{aligned} \tag{2.25}
$$

To define the α_i, α_{ij}, γ_{ii}, γ_{ij}, and ψ_i, we gather terms in (2.24) and map them to (2.25). thus gives:

$$
A = \begin{bmatrix}
-\alpha_{11} & \alpha_{12} & \cdots & \alpha_{1N} \\
\alpha_{21} & -\alpha_{22} & \alpha_{23} & \alpha_{2N} \\
\vdots & \vdots & -\alpha_{33} & \vdots \\
\alpha_{N1} & \alpha_{N2} & \cdots & -\alpha_{NN}
\end{bmatrix} \tag{2.26}
$$

$$\Gamma = \begin{bmatrix} \gamma_{11} & \gamma_{12} & \cdots & \gamma_{1N} \\ \gamma_{21} & \gamma_{22} & \gamma_{23} & \gamma_{2N} \\ \vdots & \vdots & \vdots & \vdots \\ \gamma_{N1} & \gamma_{N2} & \cdots & \gamma_{NN} \end{bmatrix}$$

$$\Psi = \begin{bmatrix} \psi_{11} & & & \\ & \ddots & & \\ & & & \psi_{NN} \end{bmatrix} \tag{2.27}$$

(2.28)

with

$$\alpha_{ii} = \lambda_{\min}(Q_i) - \delta - \sum_{j \in N_i} 2\delta + \frac{1}{\delta} \left\| 2\bar{A_i}^T P_i E_i \right\|^2 \tag{2.29}$$

$$\begin{aligned} \alpha_{ij} = & \frac{1}{\delta} \left\| 2\bar{A_i}^T P_i \bar{A_j} \right\|^2 \\ & + \frac{1}{\delta} \left\| 2 + \frac{1}{\delta} \left\| 2K_i^T C_i^T B_i^T P_i \bar{A_i} \right\|^2 C_i^T L_{ij}^T B_i^T P_i \bar{A_j} \right\|^2 \\ & + \left\| \bar{A_j}^T P_i \bar{A_j} \right\|^2 \end{aligned} \tag{2.30}$$

$$\begin{aligned} \gamma_{ii} = & \frac{1}{\delta} \left\| 2\bar{A_i}^T P_i B_i K_i C_i \right\|^2 \\ & + \sum_{j \in N} \frac{1}{\delta} \left\| 2\bar{A_i}^T P_i B_i L_{ij} C_j \right\|^2 \\ & + \left\| C_i^T K_i^T P_i B_i K_i C_i \right\| + \sum_{j \in N} 3\delta \end{aligned} \tag{2.31}$$

$$\begin{aligned} \gamma_{ij} = & \frac{1}{\delta} \left\| 2C_i^T K_i^T B_i^T P_i B_i L_{ij} C_j \right\|^2 \\ & + \frac{1}{\delta} \left\| 2C_j^T L_{ij}^T B_i^T P_i B_i L_{ij} C_j \right\|^2 \end{aligned}$$

$$+\frac{1}{\delta}\left\|2C_i^T L_{ij}^T B_i^T P_i E_i\right\|^2$$

$$\psi_{ii} = 2\delta + \sum_{j\in N} 2\delta + \left\|E_i^T P_i E_i\right\| \tag{2.32}$$

Selecting $\delta > 0$ to satisfy $\alpha_i > 0$ and the minimum eigenvalue of Q_i refers as $\lambda_{min}(Q_i)$, i is the the i-th subsystem.

Let combine the vectors as follows:

$$\begin{aligned}
V_{vec}(x_i(k)) &:= [V_1(x_1(k)), V_2(x_2(k)), \ldots, V_N(x_N(k))]^T \\
\|x(k)\|_{vec} &:= \left[\|x_1(k)\|^2, \|x_2(k)\|^2, \ldots, \|x_N(k)\|^2\right]^T \\
\|e(k)\|_{vec} &:= \left[\|e_1(k)\|^2, \|e_2(k)\|^2, \ldots, \|e_N(k)\|^2\right]^T \\
\|f_i\|_{vec} &:= \left[\|f_1\|^2, \|f_2\|^2, \ldots, \|f_N\|^2\right]^T \\
\|C_i\|_{vec} &:= \left[\|C_1\|^2, \|C_2\|^2, \ldots, \|C_N\|^2\right]^T
\end{aligned}$$

The inequality (2.25) could be compactly rewritten as:

$$\Delta V_i(x_i(k)) \leq A\|x(k)\|_{vec} + \Gamma\|e(k)\|_{vec} + \Psi\|f_i\|_{vec} \tag{2.33}$$

Assuming the spectral radius satisfies $r(A_{ii}^{-1}A_{ij}) < 1$ then,there is a $\mu > 0 \in \mathbb{R}^{N^+}$ such that $\mu^T A < 0$ [70]. The Lyapunov function selected as $V(x(k)) := \mu^T V_{vec}(x_i(k))$. Then ΔV yields:

$$\begin{aligned}
\Delta V(x(k)) &= \mu^T \Delta V_{vec}(x_i(k)) \\
&\leq \mu^T A\|x(k)\|_{vec} + \mu^T \Gamma\|e(k)\|_{vec}
\end{aligned} \tag{2.34}$$

$$+\mu\Psi \left\| f_i \right\|_{vec}$$

Assumption 4 *The demand load f_i directly affects the frequency of the power generation unit [71], which represented by the output in our model $y = C_i x_i(k)$ as described in Section 2. So, for small f_i we assume that*

$$\begin{aligned} f_i \ &:\leq \ \epsilon\Delta\omega \\ &\epsilon C_i X_i(k) \end{aligned} \tag{2.35}$$

where ϵ is a positive or negative depend on the loads type if capacitive or inductive loads.

from (2.36) and (2.35) we can rewrite (2.35) as:

$$\Delta V(x(k)) \leq -L \left\| x(k) \right\|_{vec} + J \left\| e(k) \right\|_{vec} \tag{2.36}$$

where $L := \mu^T(A + \bar{\Psi})$ and $J := \mu^T\Gamma$ are row vectors.noticing that $\mu^T A < 0$ and $\bar{\Psi} := \epsilon C_i \Psi$.

Since,l_i and j_i are an entry of L and J vectors. So, we rewrite (2.36 as follows:

$$\begin{aligned} \Delta V(x(k)) \ &\leq \ \sum_{j\in N} l_i \left\| x_i(k) \right\|^2 + \sum_{j\in N} j_i \left\| e_i(k) \right\|^2 \\ &= \ -\sum_{j\in N} \left(l_i \left\| x_i(k) \right\|^2 - j_i \left\| e_i(k) \right\|^2 \right) \end{aligned} \tag{2.37}$$

leading to asymptotic stability with $\sigma_i < \sqrt{\frac{l_i}{j_i}}$ ∎

2.3.3 Stability analysis of a MAIPS subject to transmission delay

To achieve the asymptotic stability of the MAIPS in the normal situation with a Round-robin protocol, we investigate selecting σ_i to deal with the error limits. However, the MAIPS stability is unguaranteed if the system is under the transmission delay. Our aim in this part is to address the stability of the MAIPS subject to transmission delay.

Theorem 2.3 *A multi-area interconnected power system (MAIPS) consists of N area as described in (1.1). The static feedback controller as in (2.6) is applied to control the frequency of MAIPS. Also, a sampling interval Δ satisfying Assumption 3. The MAIPS under the influence of the transmission delay with frequency and duration satisfying Assumption (2. this system is asymptotically stable if*

$$f_d + \Delta_* d_{max} < 1; \quad , \omega_1 < 1 \tag{2.38}$$

where

$$\omega_1; = \min \left\{ \frac{l_i - \sigma_i^2 j_i}{\lambda_{\max}(P_i)\mu_i} \right\}, \tag{2.39}$$

and $\Delta_* = N\Delta$, l_i, j_i, μ_i, and σ_i are as in lemma 2.1.

Proof. Theorem 2.3 proof is expressed in two main steps:

1. No delay periods.

   From assumption 3,and (2.9) where σ_i satisfying Lemma 2.1 and (2.37) < 0. The Lyapunov function derivative is given as :

$$\begin{aligned} \Delta V(x(k)) &\leq -\sum_{j\in N}\left(l_i - j_i\sigma_i^2\right)\|x_i(k)\|^2 \\ &\leq -\sum_{j\in N}\frac{l_i - j_i\sigma_i^2}{\lambda_{max}(P_i)\mu_i}\mu_i V_i \\ &\triangleq -\omega_1 V(x(k)) \end{aligned} \tag{2.40}$$

   where $\omega_1 ;= \min\{\frac{l_i-\sigma_i^2 j_i}{\lambda_{\max}(P_i)\mu_i}\}$. So, for $k \in [h_n + \tau_n, T_{n+1}[$ (no delay period), the Lyapunov function rewritten as:

$$V(x(k)) \leq (1-\omega_1)^{k-h_n-\tau_n} V(x(h_n+\tau_n)) \tag{2.41}$$

2. During delay.

   Introducing z_m^i as the last attempt successfully transmitted on the channel prior to the Trans. By considering $e_i(k)$ as mentioned previously, this leads to

$$e_i(k) = x_i(z_m^i) - x_i(k) = x_i(h_n) - x_i(k) \tag{2.42}$$

   and

$$\begin{aligned} \|e_i(k)\|^2 &\leq \|x_i(h_n)\|^2 + 2\|x_i(k)\|\,\|x_i(h_n)\| + \|x_i(k)\|^2 \\ &\leq 2\|x_i(h_n)\|^2 + 2\|x_i(k)\|^2 \end{aligned} \tag{2.43}$$

for $k \in H_n$. If $\|e_i(k)\|^2$ for $i \in N$, we will lead to

$$\sum_{i \in N} \|e_i(k)\|^2 \leq 2 \sum_{i \in N} \|x_i(h_n)\|^2 + 2 \sum_{i \in N} \|x_i(k)\|^2 \tag{2.44}$$

If $\sum_{i \in N} \|x_i(h_n)\|^2 \leq \sum_{i \in N} \|x_i(k)\|^2$ we have that $\sum_{i \in N} \|e_i(k)\|^2 \leq 4 \sum_{i \in N} \|x_i(k)\|^2$. Otherwise, we have $\sum_{i \in N} \|e_i(k)\|^2 \leq 4 \sum_{i \in N} \|x_i(h_n)\|^2$

Calling (2.37), we can conclude that

$$\Delta V(x(k)) \leq \sum_{j \in N} j_i \|e_i(k)\|^2 \tag{2.45}$$

Thus, for all $k \in H_n$ (transmission delay interval) If $\sum_{i \in N} \|x_i(h_n)\|^2 \leq \sum_{i \in N} \|x_i(k)\|^2$, the difference of the Lyapunov function rewritten as:

$$\begin{aligned} \Delta V(x(k)) &\leq \max\{j_i\} \sum_{j \in N} \|e_i(k)\|^2 \\ &\leq 4\max\{j_i\} \sum_{j \in N} \|x_i(k)\|^2 \\ &\leq \frac{4\max\{j_i\}}{\min\{\mu_i \lambda_{min}(P_i)\}} \sum_{j \in N} \mu_i V(x_i(k)) \\ &\triangleq \omega_2 V(x(k)) \end{aligned} \tag{2.46}$$

with $\omega_2 := \frac{4\max\{j_i\}}{\min\{\mu_i \lambda_{min}(P_i)\}}$. Also, $\forall k \in H_n$ with $\sum_{i \in N} \|x_i(h_n)\|^2 > \sum_{i \in N} \|x_i(k)\|^2$, one has

$$\Delta V(x(k)) \leq \omega_2 V(x(h_n)) \tag{2.47}$$

So, (2.46) and (2.47) implying that the Lyapunov function in the transmission delay period H_n satisfy the following equation

$$V(x(k)) \leq (1+\omega_2)^{k-h_n} V(x(h_n)) \tag{2.48}$$

During the transaction between stable and unstable modes.we will reflect the the protocol waiting time, the Lyapunov function in this instant $V(x(k)) \leq (1-\omega_1)^{k-h_n-\tau_n-N\Delta} V(x(h_n+\tau_n+N\Delta))$ for $t \in [h_n+\tau_n+N\Delta, T_{n+1}[$ and $V(x(k)) \leq (1+\omega_2)^{k-h_n} V(x(h_n))$ for $t \in [h_n, h_n+\tau_n+N\Delta[$.

In conclusion, the overall behavior of the closed-loop system could be treated as a switching system with two modes. So, when simple iterations are applied to the Lyapunov function in and out of the presence of the transmission delay status, we will get

$$V(x(k)) \leq (1-\omega_1)^{[k-\kappa_*-(f_d+\Delta_* d_{max})k]} (1+\omega_2)^{[\kappa_*+(f_d+\Delta_* d_{max})k]} V(x(0)) \tag{2.49}$$

To assure the stability of the last equation, (2.38) is obtained easily.

∎

Remark 7 *Theorem 2.3 offer a criterion to characterize the stability of distributed system in the form of (1.1) with an output feedback controller in the form of (2.6) and in the presence of transmission delay. The transmission delay is assumed to have constrained frequency and duration as described in Assumption 2. The signals are exchanged over a communication channel with sampling interval Δ satisfying*

Assumption 3.

Remark 8 *The stability of the MAIPS is affected by the sampling interval (Δ) of the Round-robin protocol since it delimits when the overall system is able to repair communication. In the case where the bounded duration and frequency of the transmission delay subjected to the MAIPS with applying appropriate Round-robin inter-sampling time diminish the left-hand side of (2.38) that ensure the stability of the MAIPS. However, this is at the expense of high communication facilities.*

2.4 Simulation

A simulation result of three scenarios are shown in this section. The interconnected power system described in section (1.2) with the typology illustrated in 2.1 is tested with following parameters. The system parameters used in the simulation is listed in table 2.1. The controller gain calculated using YALMIP as follows:

$$\begin{aligned} K_1 &= -1.376, K_2 = -2.433, K_3 = 0.852 \\ L_{12} &= -4.145, \quad L_{13} = -0.5034 \\ L_{21} &= -0.35, \quad L_{23} = -2.96 \\ L_{31} &= -0.671, \quad L_{32} = 0.482 \end{aligned} \tag{2.50}$$

In the three scenarios a step load change (0.1 p.u.) is applied at time = 0.8s.

Table 2.1: Areas parameters

Parameter	Area (1)	Area (2)	Area (3)
M_i^a	3.5	4.0	3.75
R_i^f	0.03	0.07	0.05
D_i	2	2.75	2.4
R_i	1	1	1
T_{CHi}	50	10	30
T_{G1}	40	25	32
B_i	1	1	1
T_{ij}	$T_{12} = T_{13} = 7.54$	$T_{21} = T_{23} = 7.54$	$T_{31} = T_{32} = 7.54$

2.4.1 Designed controller in Nominal Situation

As shown in **Figure (2.2)** the MAIPS is stable in a normal situation with the controller gain in (2.50). The applied controller is able to return the deviation of the frequency to zero whenever the load fluctuates. In this case, the load change is occurring at time 8s.

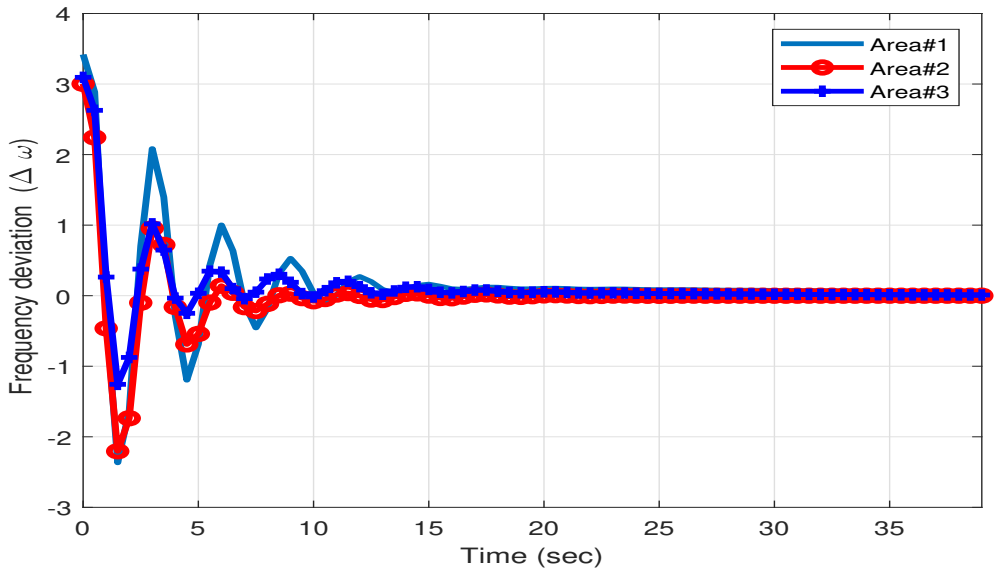

Figure 2.2: The output of the system in the nominal situation with the designed controller

2.4.2 Under transmission delay

In this scenario, a transmission delay was implemented on the system with the assumption 2. In **Figure 2.3** the three interconnected power system is illustrated under the transmission delay characterized in section 2.2.

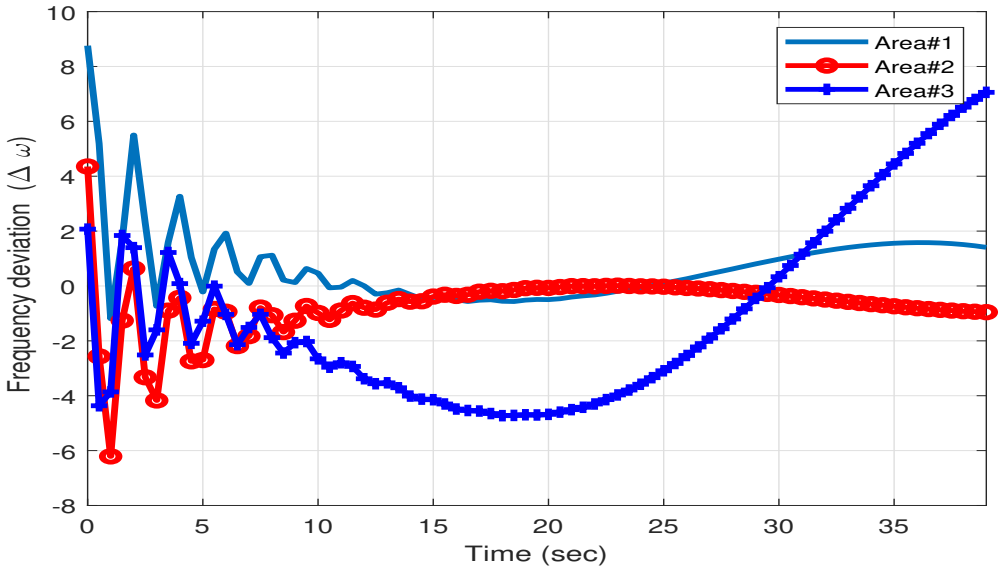

Figure 2.3: The output of the system under transmission delay using the nominal T_s

2.4.3 Stabilization under transmission delay

Using Lemma 2.1 and YALMIP,we found the follows:

$$P_1 = 10^{-6} \times \begin{bmatrix} 6.634 & 43.23 & -2.544 & 6049.83 \\ 24.22 & 2.756 & -23.245 & -4.761 \\ -5.674 & -14.275 & 4.79 & -84.784 \\ 549.80 & -4.51 & -12.73 & 8.004 \end{bmatrix}$$

$$P_2 = 10^{-6} \times \begin{bmatrix} 6.113 & 45.95 & -4.256 & 42.594 \\ 30.95 & 3.658 & -3.674 & -3.5485 \\ -2.668 & -20.674 & 1.8964 & -322.71 \\ 72.174 & -4.0481 & -263.71 & 8.976 \end{bmatrix},$$

$$P_3 = 10^{-6} \times \begin{bmatrix} 5.0538 & 2.467 & -2.035 & 60.134 \\ 62.462 & 2.5692 & -21.324 & -2.7112 \\ -2.063 & -20.618 & 2.5825 & -441.62 \\ 26.423 & -2.578 & -46.2 & 7.3178 \end{bmatrix},$$

$$
\begin{aligned}
Q_1 &= 10^{-7} \times \begin{bmatrix} 45.023 & 54.6235 & 5.257 & 5.1677 \\ 5.6775 & 7.3609 & 6.2751 & 5.7078 \\ 6.5657 & 2.2751 & 4.0092 & 5.8730 \\ 6.1737 & 4.7348 & 1.0630 & 6.5553 \end{bmatrix}, \\
Q_2 &= 10^{-5} \times \begin{bmatrix} 45.2651 & 6.7758 & 20.8955 & 9.1632 \\ 4.0258 & 6.1497 & 8.1212 & 2.011 \\ 3.5455 & 7.1612 & 6.2509 & 5.7868 \\ 5.1653 & 2.7691 & 14.3668 & 1.8793 \end{bmatrix}, \\
Q_3 &= 10^{-5} \times \begin{bmatrix} 45.918 & 3.6566 & 5.1118 & 6.1551 \\ 5.7346 & 7.4899 & 6.2784 & 7.2669 \\ 0.2918 & 3.2184 & 5.2896 & 9.7211 \\ 2.1556 & 3.2376 & 3.7213 & 3.4172 \end{bmatrix}
\end{aligned}
$$

Then we obtain:

$$A = 10^{-6} \times \begin{bmatrix} 0.402 & 0.546 & 0.235 \\ 0.084 & 0.384 & 0.348 \\ 0.170 & 0.097 & 0.656 \end{bmatrix}$$

$$\Gamma = 10^{-6} \times \begin{bmatrix} 0.481 & 0.284 & 0.355 \\ 0.366 & 0.766 & 0.144 \\ 0.367 & 0.902 & 0.886 \end{bmatrix},$$

$$\Psi = 10^{-8} \times \begin{bmatrix} 0.654 & 0 & 0 \\ 0 & 0.557 & 0 \\ 0 & 0 & 0.364 \end{bmatrix}$$

Since the σ_1, σ_2 and σ_3 are (0.869), (1.002) and (0.972), respectively. the σ, in this case, is chosen to be (0.8). Based on Assumption 3, we select the sampling interval $\Delta = 0.25$s. From this we calculate ω_1,ω_2 and ω_3 to be $(3.004(10)^4)$,and (1.458), respectively. As shown in **Figures 2.5**, the designing parameters able to maintain the stability of the MAIPS in the presence of the DoS attack and stable the frequency to the nominal state.

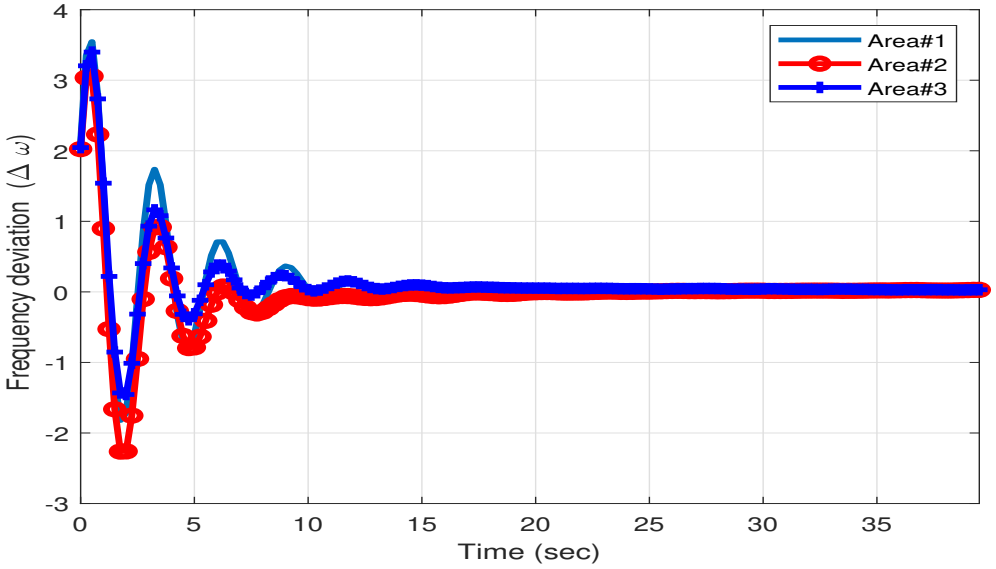

Figure 2.4: The output of the system in the nominal situation using the modified T_s

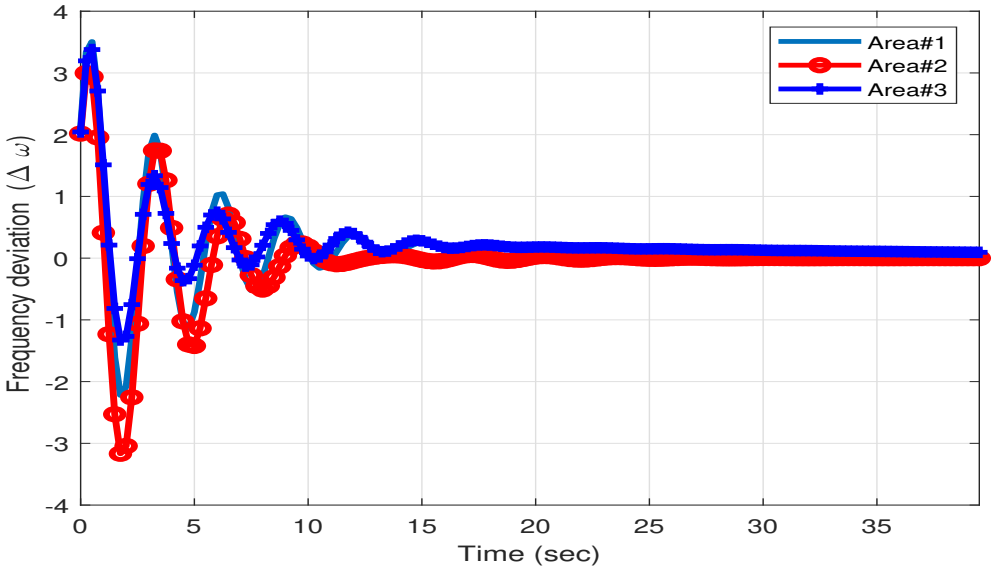

Figure 2.5: The output of the system under transmission delay using the modified T_s

CHAPTER 3

STABILITY ANALYSIS UNDER DANIAL OF SERVICE (DOS) ATTACK

3.1 Introduction

Recently, researchers widely used the small gain approached to solve the stabilization problem of distributed systems. To maintain the stability of large-scale systems in the presence of a limited communication medium, an event-triggered sampling scheme was examined with distributed controllers in [23]. Also, the initial state is assured to be restored for a complex systems in the case of mixed attacks in independent transmitting channels, Song et al. proposed a robust pinning synchronization control problem [24]. a hierarchical game method was presented in [25] for sovling the control challenge of a wireless networked control system affected by DoS attack.

This work is an extension of [72], where The challenge in this subject is to design a method and a parameter based on the output signals that guarantee the stability of a MAIPS in the presence of a DoS attack. The contribution of this chapter can be summarized as follows:

- We implement the output feedback controller to stabilize a MAIPS with load deviation in the normal situation when there is not any DoS attack.
- The limits on the frequency and duration of the DoS attacks are characterized for a MAIPS that implements a typical Round robin communication protocol.
- The stability of a discrete time MAIPS is discussed and analyzed such that the the stability is maintained in the presence of DoS attack.
- An illustrative example of a typical MAIPS is provided with several scenarios considering the nominal controller with the typical and the modified sampling time in the absent and presence of a DoS attack to verify the effectiveness of the proposed approach.

Considering the MAIPS described by model (1.1). the target is to design an appropriate control algorithm to guarantee the close loop stability of all areas on the power network. N in the model is representing the set of the neighbor's agent j. In this manner, the controller proposes to use the data of the subsystem and its connected neighbors to compute the input control signals for each time step as a distributed system. The controller aims to ensure the stability of the MAIPS. the diagram of the system with three areas was shown in **Figure 3.1**.

The remaining of the chapter is organized as follows: The modeling of a MAIPS is presented in Section 1.2. In Section 3.2, the framework is provided. Then, the stability analysis of a MAIPS is discussed in Section 3.3. The simulation of an illustrative example is presented in Section 3.4.

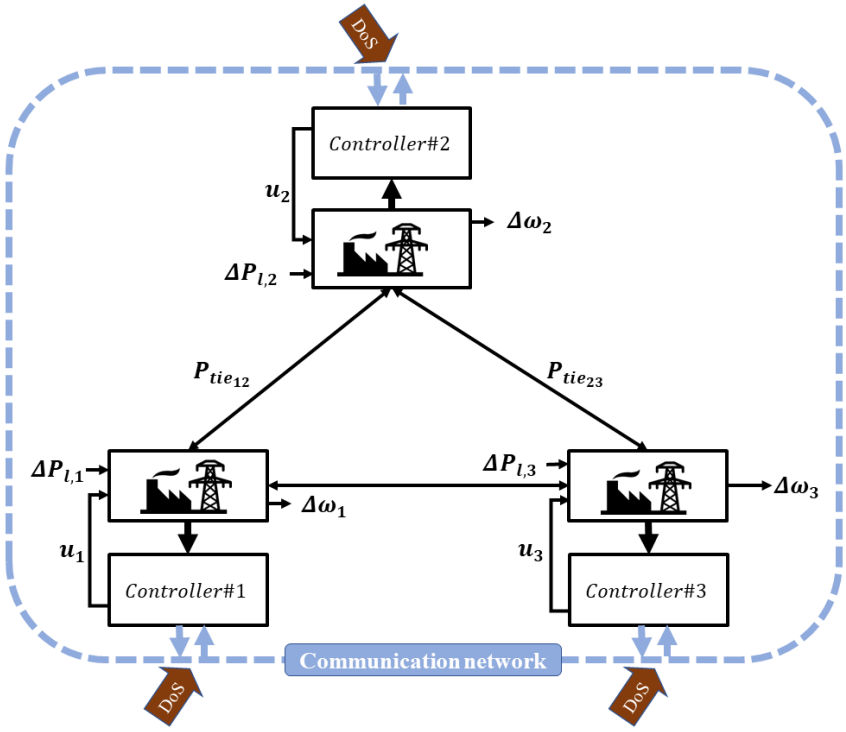

Figure 3.1: Three-area Interconnected Power System

3.2 Framework

Let consider the discrete MAIPS expressed in section (1.2). The (1.1) is the mathematical model of MAIPS that employing the communication network to transfers the data and measurements among each area. A controller related these measurements to figure the desirable control signals and forward them to the actuators of the systems to maintain a certain frequency of the grid at the desired frequency. In this work,

we assume that the Round-Robin protocol is reflected in a communication network. So, the signals arrive at each unit in the system in a sample-and-hold manner.For example, $y_i(k_i')$ where k_i' illustrates series of communication attempts.

Remark 9 *We assume the static output feedback gains K_i are existed that press all eigenvalues of matrix $\bar{A}_i = A_i + B_i K_i C_i$ to have norm strictly less than one, i.e. each feedback area is Schur stable.*

Remark 10 *Each control input u_i affecting subsystem i consists of two parts. The first part depends on the self output with a gain of K_i, and the other depends on the neighbors' output with a gain of L_{ij}, such that*

$$u_i(k) \quad = \quad K_i C_i x_i(k_i') + \sum_{j \in N_i} L_{ij} C_j x_j(k_i') \tag{3.1}$$

3.2.1 DoS attacks Characteristics

In this chapter, a failure in sending or receiving signals has been considered as a DoS attack. The failure caused by channel unavailability or by attackers is studied. The DoS attacks consequently affect the transmission attempts of all connected areas.

Similar to [73], [19], the DoS attacks model, in this work, has bounded duration and frequency. $\{H_n\}_{n \in \mathbb{N}_0}, h_0 \geq 0$, denote series of the DoS attacks. In other words, the DoS is executed or not executed (one or zero). Where the n denotes the n-th DoS with a length $\tau_n \in \mathbb{N}0$ could be rewritten as:

$$H_n := \{h_n\} \cup [h_n, h_n + \tau_{n-1}] \tag{3.2}$$

When $\tau_n = 0$, H_n is presented as a pulse signal at h_n. If $\tau_n \neq 0$,$[h_n, h_n + \tau_{n-1}]$ denotes an interval from the time h_n (include h_n) to $(h_n + \tau_{n-1})$. In parallel, $[\tau, k-1]$ denotes an interval from τ to $k-1$. Assume $\tau, k \in \mathbb{N}_0$ with $k \geq \tau$, let $n(\tau, k)$ refers to the n-th DoS attacks along $[\tau, k-1]$, also $\Xi(\tau, k)$ refers to the subsections of $[\tau, k]$ when the DoS influence the system given:

$$\Xi(\tau, k) := \bigcup_{n \in \mathbb{N}_0} T_n \cap [\tau, k] \tag{3.3}$$

Also, $\Theta(\tau, k)$ denotes the time interval when the DoS attack is inactive on the system. it could be rewritten as follows:

$$\Theta(\tau, k) := [\tau, k] \backslash \Xi(\tau, k) \tag{3.4}$$

In [66], [23] authors illustrate that present secure control designs cannot handle and treat the general patterns of cyber attacks efficiently. In this manner, we study a class of cyber attacks patterns under the following assumptions:

Assumption 5 *(The DoS attack frequency). Assuming constants $\eta \in \mathbb{N}$ and $\tau_D \in \mathbb{N}_+$ that satisfied the following:*

$$n(\tau, k) \leq \eta + \frac{k - \tau}{\tau_D} \tag{3.5}$$

for all $\tau, k \in \mathbb{N}$ *with* $k \geq \tau$.

Assumption 6 *(The duration of the DoS attack). Assume that constants* $\kappa \in \mathbb{N}$ *and* $T \in \mathbb{N} > 1$ *is existing such that*

$$|\Xi(\tau, k)| \leq \kappa + \frac{k - \tau}{T} \tag{3.6}$$

for all $\tau, k \in \mathbb{N} \geq 0$ *with* $k \geq \tau$.

3.3 Stability analysis

The aim is to administrate the stability of the MAIPS in the normal situation or with the presence of the DoS attacks. Mainly we address the stabilization problem of MAIPS connected by tie-line in the nominal situation and under Dos Attack influence.

At each transmission instant, Let $e_i(k)$ refer to the error between the transmitted states $x_i(k_i')$ and the actual states $x_i(k)$ in each i-area. So, it could be written as:

$$e_i(k) = x_i(k_i') - x_i(k), \quad i = 1, 2, \ldots, N \tag{3.7}$$

The system dynamic of *an*-area could be characterized by integrating the (1.1),

(3.1) and (3.7) such that

$$\begin{aligned} x_i(k+1) &= \bar{A}_i x_i(k) + B_i K_i C_i e_i(k) + E_i \Delta P_{Li} \\ &\quad + B_i \sum_{j \in N_i} L_{ij} C_j e_j(k) + \sum_{j \in N_i} \bar{A}_j x_j(k) \end{aligned} \tag{3.8}$$

where $\bar{A}_i = \bar{A}_i + B_i K_i C_i, \bar{A}_j = \bar{A}_j + B_i L_{ij} C_j$. From equation (1.1), the states of the connected neighbors are affecting the dynamic system.

Remark 11 *As illustrated in (3.8) the stability can be achieved in a weak couplings situation and within a small error e. Besides, a design parameter σ has been introduced to clarify the "smallness" of e.*

Assumption 7 *(Inter-sampling interval). With nonexistence DoS attacks there is an inter-sampling interval (Δ) satisfying:*

$$\|e_i(k)\| \leq \sigma_i \|x_i(k)\| \tag{3.9}$$

σ_i here is holds as a design factor.

Remark 12 *Even if Δ is not shown explicitly in (3.9), it can be noticed from the definition of the error (3.7) that the inter-sampling interval affect the stability of the system. Referring to Remark 11, Assumption 7 guarantees the "smallness" of the error by selecting a proper inter-sampling interval.*

Remark 13 *It is worth to mention that the designing of the inter-sampling interval, Δ in (3.9) is a considerable problem. An inter-sampling interval satisfying limits as*

(3.9) could be precisely resolved for centralized settings [66]. While some literature computes and applies a lower bound of time elapsed between two events to avoid Zeno behavior in asymptotically stable distributed/decentralized systems [67], [68].

According to [66], the selection and design of Δ and σ_i is essential to guarantee the stability of the distributed systems.

3.3.1 A small-gain approach for a MAIPS

By choosing the Lyapunov function $V_i(k) = x_i^T(k)P_i x_i(k)$ where $Q_i = Q_i^T > 0$, and P_i is the the unique solution of the Lyapunov equation $\bar{A}_i^T P_i \bar{A}_i - P_i + Q_i = 0$. Then each subsystem i should satisfy:

$$\lambda_{\min}(P_i)\|x_i(k)\|^2 \leq V_i(x_i(k)) \leq \lambda_{\max}(P_i)\|x_i(k)\|^2 \tag{3.10}$$

thus $\lambda_{\min}(P_i)$ is the smallest eigenvalue of of P_i and $\lambda_{\max}(P_i)$ is the largest. To maintain the stability of the system, σ_i must be selected base on lemma (3.1).

Lemma 3.1 *For MAIPS described by (1.1) that controlled by (3.1). Let $\mu \in \mathbb{R}_+^N$ to be any column vector satisfy $\mu^T A < 0$. Then, the MAIPS is asymptotically stable if there is $\sigma_i \forall i \in N$ such that*

$$\sigma_i < \sqrt{\frac{l_i}{j_i}} \tag{3.11}$$

Where for l_i refers to the i-th vector of $L := \mu^T(-A + \bar{\Psi})$and j_i refers to the j-th vector $J := \mu^T\Gamma$. The matrices A, Γ and Ψ are defined below.

Proof.

The Lyapunov function is formed in order to establish the main theorem is

$$V_i(k) = x_i^T(k)P_ix_i(k) \tag{3.12}$$

Now, let evaluate $\Delta VIs)$ as follows:

$$\begin{aligned}
\Delta V_i(k) &= V_i(k+1) - V_i(k) \\
\Delta V_i(k) &= x_i^T(k)(\bar{A}_i^T P_i \bar{A}_i - P_i)x_i(k) + 2x_i^T(k)\bar{A}_i^T P_i B_i K_i C_i e_i(k) \\
&\quad +2x_i^T(k)\bar{A}_i^T P_i \sum_{j\in N} B_i L_{ij} C_j e_i(k) + 2x_i^T(k)\bar{A}_i^T P_i E_i \Delta P_{Li} \\
&\quad +2x_i^T(k)\bar{A}_i^T P_i \sum_{j\in N} \bar{A}_j x_j(k) + e_i^T(k)C_i^T K_i^T B_i^T P_i B_i K_i C_i e_i(k) \\
&\quad +2e_i^T(k)C_i^T K_i^T B_i^T P_i \sum_{j\in N} B_i L_{ij} C_j e_i(k) + 2e_i^T(k)K_i^T C_i B_i^T P_i E_i \Delta P_{Li} \\
&\quad +2e_i^T(k)C_i^T K_i^T B_i^T P_i \sum_{j\in N} \bar{A}_j x_j(k) + \sum_{j\in N} e_j^T(k)L_{ij}C_j B_i^T P_i B_i L_{ij} e_j(k) \\
&\quad +2\sum_{j\in N} e_j^T(k)L_{ij}C_j B_i^T P_i E_i \Delta P_{Li} + 2\sum_{j\in N} e_j^T(k)L_{ij}C_j B_i^T P_i \bar{A}_j x_j(k) \\
&\quad +\delta {P_{Li}}^T E_i^T P_i E_i \Delta P_{Li} + 2\delta {P_{Li}}^T E_i^T P_i \sum_{j\in N} \bar{A}_j x_j(k) \\
&\quad +\sum_{j\in N} x_i^T(k){\bar{A}_j}^T P_i \bar{A}_j x_j(k)
\end{aligned} \tag{3.13}$$

Hence, the compact form is given as:

$$\Delta V_i(k) = \Omega_i^T(k)\Lambda_i\Omega_i(k) < 0 \tag{3.14}$$

where

$$\Omega_i^T(k) = \begin{bmatrix} e_i(k) & x_i(k) & \sum_{j\in N_i} e_j(k) & \sum_{j\in N_i} x_j(k) & \Delta P_{Li} \end{bmatrix}^T \tag{3.15}$$

The difference equation (3.13) could be described by taken the norm as following:

$$\begin{aligned}
\Delta V_i(k) \;=\; & -\lambda(Q_i)\left\|x_i(k)\right\|^2 + \left\|2\bar{A}_i^T P_i B_i K_i C_i\right\| \left\|x_i^T(k)\right\| \left\|e_i(k)\right\| \\
& + \left\|2\bar{A}_i^T P_i \sum_{j\in N} B_i L_{ij} C_j\right\| \left\|x_i^T(k)\right\| \left\|e_i(k)\right\| + \left\|2\bar{A}_i^T P_i E_i\right\| \left\|x_i^T(k)\right\| \left\|\Delta P_{Li}\right\| \\
& + \left\|2\bar{A}_i^T P_i \sum_{j\in N} \bar{A}_j\right\| \left\|x_i^T(k)\right\| \left\|x_j(k)\right\| + \left\|C_i^T K_i^T B_i^T P_i B_i K_i C_i\right\| \left\|e_i(k)\right\|^2 \\
& + \left\|2C_i^T K_i^T B_i^T P_i \sum_{j\in N} B_i L_{ij} C_j\right\| \left\|e_i^T(k)\right\| \left\|e_i(k)\right\| + \left\|2C_i^T K_i^T B_i^T P_i E_i\right\| \left\|e_i^T(k)\right\| \left\|\Delta P_{Li}\right\| \\
& + \left\|2K_i^T C_i B_i^T P_i \sum_{j\in N} \bar{A}_j\right\| \left\|e_i^T(k)\right\| \left\|x_j(k)\right\| + \left\|\sum_{j\in N}(k) L_{ij} C_j B_i^T P_i B_i L_{ij}\right\| \left\|e_j^T\right\| \left\|e_j(k)\right\| \\
& + \left\|2\sum_{j\in N} L_{ij} C_j B_i^T P_i E_i\right\| \left\|\Delta P_{Li}\right\|^2 + \left\|2\sum_{j\in N} L_{ij} C_j B_i^T P_i \bar{A}_j\right\| \left\|e_j^T(k)\right\| \left\|x_j(k)\right\| \\
& + \left\|E_i^T P_i E_i\right\| \left\|\Delta P_{Li}\right\|^2 + \left\|2E_i^T P_i \sum_{j\in N} \bar{A}_j\right\| \left\|\delta {P_{Li}}^T\right\| \left\|x_j(k)\right\| \\
& + \left\|\sum_{j\in N} {\bar{A}_j}^T P_i \bar{A}_j\right\| \left\|x_j(k)\right\|^2
\end{aligned} \tag{3.16}$$

By utilizing Young's inequalities, assuming Z, V, and J any matrices with $\delta > 0$

consequently

$$\|Z\| \|V\| \|J\| \leq \delta \|V\|^2 + \frac{1}{\delta} \|Z\|^2 \|J\|^2 \tag{3.17}$$

By utilizing the inequalities (3.17) on (3.17) lead to:

$$\begin{aligned} \Delta V_i(x_i(k)) \leq & -\alpha_{ii} \|x_i(k)\|^2 + \psi \|\Delta P_{Li}\| + \sum_{j \in N_i} \alpha_{ij} \|x_j(k)\|^2 \\ & + \gamma_{ii} \|e_i(k)\|^2 + \sum_{j \in N_i} \gamma_{ij} \|e_j(k)\|^2 \end{aligned} \tag{3.18}$$

To define the α_i, α_{ij}, γ_{ii}, γ_{ij}, and ψ_i, we gather terms in (3.17) and map them to (3.18). thus gives:

$$A = \begin{bmatrix} -\alpha_{11} & \alpha_{12} & \cdots & \alpha_{1N} \\ \alpha_{21} & -\alpha_{22} & \alpha_{23} & \alpha_{2N} \\ \vdots & \vdots & -\alpha_{33} & \vdots \\ \alpha_{N1} & \alpha_{N2} & \cdots & -\alpha_{NN} \end{bmatrix} \tag{3.19}$$

$$\Gamma = \begin{bmatrix} \gamma_{11} & \gamma_{12} & \cdots & \gamma_{1N} \\ \gamma_{21} & \gamma_{22} & \gamma_{23} & \gamma_{2N} \\ \vdots & \vdots & \vdots & \vdots \\ \gamma_{N1} & \gamma_{N2} & \cdots & \gamma_{NN} \end{bmatrix}$$

$$\Psi = \begin{bmatrix} \psi_{11} & & & \\ & \ddots & & \\ & & & \psi_{NN} \end{bmatrix} \tag{3.20}$$

(3.21)

with

$$\alpha_{ii} = \lambda_{\min}(Q_i) - \delta - \sum_{j \in N_i} 2\delta + \frac{1}{\delta} \left\| 2\bar{A_i}^T P_i E_i \right\|^2 \tag{3.22}$$

$$\begin{aligned} \alpha_{ij} = & \frac{1}{\delta} \left\| 2\bar{A_i}^T P_i \bar{A_j} \right\|^2 \\ & + \frac{1}{\delta} \left\| 2 + \frac{1}{\delta} \left\| 2K_i^T C_i^T B_i^T P_i \bar{A_i} \right\|^2 C_i^T L_{ij}^T B_i^T P_i \bar{A_j} \right\|^2 \\ & + \left\| \bar{A_j}^T P_i \bar{A_j} \right\|^2 \end{aligned} \tag{3.23}$$

$$\begin{aligned} \gamma_{ii} = & \frac{1}{\delta} \left\| 2\bar{A_i}^T P_i B_i K_i C_i \right\|^2 \\ & + \sum_{j \in N} \frac{1}{\delta} \left\| 2\bar{A_i}^T P_i B_i L_{ij} C_j \right\|^2 \\ & + \left\| C_i^T K_i^T P_i B_i K_i C_i \right\| + \sum_{j \in N} 3\delta \end{aligned} \tag{3.24}$$

$$\begin{aligned} \gamma_{ij} = & \frac{1}{\delta} \left\| 2C_i^T K_i^T B_i^T P_i B_i L_{ij} C_j \right\|^2 \\ & + \frac{1}{\delta} \left\| 2C_j^T L_{ij}^T B_i^T P_i B_i L_{ij} C_j \right\|^2 \\ & + \frac{1}{\delta} \left\| 2C_i^T L_{ij}^T B_i^T P_i E_i \right\|^2 \end{aligned}$$

$$\psi_{ii} = 2\delta + \sum_{j \in N} 2\delta + \left\| E_i^T P_i E_i \right\| \tag{3.25}$$

Selecting $\delta > 0$ to satisfy $\alpha_i > 0$ and the minimum eigenvalue of Q_i refers as $\lambda_{min}(Q_i)$, i is the the i-th subsystem.

Let combine the vectors as follows:

$$V_{vec}(x_i(k)) := [V_1(x_1(k)), V_2(x_2(k)), \ldots, V_N(x_N(k))]^T$$

$$
\begin{aligned}
\|x(k)\|_{vec} &:= \left[\|x_1(k)\|^2, \|x_2(k)\|^2, \ldots, \|x_N(k)\|^2\right]^T \\
\|e(k)\|_{vec} &:= \left[\|e_1(k)\|^2, \|e_2(k)\|^2, \ldots, \|e_N(k)\|^2\right]^T \\
\|\Delta P_{Li}\|_{vec} &:= \left[\|\Delta P_{L1}\|^2, \|\Delta P_{L2}\|^2, \ldots, \|\Delta P_{LN}\|^2\right]^T \\
\|C_i\|_{vec} &:= \left[\|C_1\|^2, \|C_2\|^2, \ldots, \|C_N\|^2\right]^T
\end{aligned}
$$

The inequality (3.18) could be compactly rewritten as:

$$
\Delta V_i(x_i(k)) \leq A \|x(k)\|_{vec} + \Gamma \|e(k)\|_{vec} + \Psi \|\Delta P_{Li}\|_{vec} \tag{3.26}
$$

Assuming the spectral radius satisfies $r(A_{ii}^{-1}A_{ij}) < 1$ then,there is a $\mu > 0 \in \mathbb{R}_+^n$ such that $\mu^T A < 0$ [70]. The Lyapunov function selected as $V(x(k)) := \mu^T V_{vec}(x_i(k))$. Then ΔV yields:

$$
\begin{aligned}
\Delta V(x(k)) &= \mu^T \Delta V_{vec}(x_i(k)) \\
&\leq \mu^T A \|x(k)\|_{vec} + \mu^T \Gamma \|e(k)\|_{vec} \\
&\quad + \mu\Psi \|\Delta P_{Li}\|_{vec}
\end{aligned} \tag{3.27}
$$

Assumption 8 *The demand load ΔP_{Li} directly affects the frequency of the power generation unit [71], which represented by the output in our model $y = C_i x_i(k)$ as described in Section 2. So, for small ΔP_{Li} we assume that*

$$
\begin{aligned}
\Delta P_{Li} &:\leq \epsilon \Delta\omega \\
&\quad \epsilon C_i X_i(k)
\end{aligned} \tag{3.28}
$$

where ϵ is a positive or negative depend on the loads type if capacitive or inductive loads.

from (3.29) and (3.28) we can rewrite (3.28) as:

$$\Delta V(x(k)) \leq -L \left\| x(k) \right\|_{vec} + J \left\| e(k) \right\|_{vec} \tag{3.29}$$

where $L := \mu^T(A + \bar{\Psi})$ and $J := \mu^T\Gamma$ are row vectors.noticing that $\mu^T A < 0$ and $\bar{\Psi} := \epsilon C_i \Psi$.

Since,l_i and j_i are an entry of L and J vectors. So, we rewrite (3.29 as follows:

$$\begin{aligned} \Delta V(x(k)) &\leq \sum_{j \in N} l_i \left\| x_i(k) \right\|^2 + \sum_{j \in N} j_i \left\| e_i(k) \right\|^2 \\ &= -\sum_{j \in N} \left(l_i \left\| x_i(k) \right\|^2 - j_i \left\| e_i(k) \right\|^2 \right) \end{aligned} \tag{3.30}$$

leading to asymptotic stability with $\sigma_i < \sqrt{\frac{l_i}{j_i}}$ ∎

3.3.2 Stability analysis of a MAIPS subject to DoS attacks

To achieve the asymptotic stability of the MAIPS in the normal situation with a Round-robin protocol, we investigate selecting σ_i to deal with the error limits. However, the MAIPS stability is unguaranteed if the system is under the DoS. Our aim in this part is to address the stability of the MAIPS subject to DoS attack.

Theorem 3.1 *A multi-area interconnected power system (MAIPS) consists of N area as described in (1.1). The static feedback controller as in (3.1) is applied to control*

the frequency of MAIPS. Also, a sampling interval Δ satisfying Assumption 7. The MAIPS under the influence of the DoS attack with frequency and duration satisfying Assumptions (5, and 6) with any η,τ_D, κ, and T. this system is asymptotically stable if

$$\frac{1}{T} + \frac{\Delta_*}{\tau_D} < 1; \quad , \omega_1 < 1 \tag{3.31}$$

where

$$\omega_1; = \min\left\{ \frac{l_i - \sigma_i^2 j_i}{\lambda_{\max}(P_i)\mu_i} \right\}, \tag{3.32}$$

and $\Delta_* = N\Delta$, l_i, j_i, μ_i, and σ_i are as in lemma 3.1.

Proof. Theorem 3.1 proof is expressed in two main steps:

1. No attacks periods.

   From assumption 7,and (3.9) where σ_i satisfying Lemma 3.1 and (3.30) < 0. The Lyapunov function derivative is given as :

$$\begin{aligned} \Delta V(x(k)) &\leq -\sum_{j\in N} \left(l_i - j_i\sigma_i^2\right) \|x_i(k)\|^2 \\ &\leq -\sum_{j\in N} \frac{l_i - j_i\sigma_i^2}{\lambda_{max}(P_i)\mu_i} \mu_i V_i \\ &\triangleq -\omega_1 V(x(k)) \end{aligned} \tag{3.33}$$

   where $\omega_1; = \min\{\frac{l_i - \sigma_i^2 j_i}{\lambda_{\max}(P_i)\mu_i}\}$. So, for $k \in [h_n + \tau_n, T_{n+1}[$ (no attack period), the

Lyapunov function rewritten as:

$$V(x(k)) \leq (1-\omega_1)^{k-h_n-\tau_n} V(x(h_n+\tau_n)) \tag{3.34}$$

2. During attacks.

Introducing z_m^i as the last attempt successfully transmitted on the channel prior to the DoS attack. By considering $e_i(k)$ as mentioned previously, this leads to

$$e_i(k) = x_i(z_m^i) - x_i(k) = x_i(h_n) - x_i(k) \tag{3.35}$$

and

$$\begin{aligned} \|e_i(k)\|^2 &\leq \|x_i(h_n)\|^2 + 2\|x_i(k)\|\|x_i(h_n)\| + \|x_i(k)\|^2 \\ &\leq 2\|x_i(h_n)\|^2 + 2\|x_i(k)\|^2 \end{aligned} \tag{3.36}$$

for $k \in H_n$. If $\|e_i(k)\|^2$ for $i \in N$, we will lead to

$$\sum_{i\in N} \|e_i(k)\|^2 \leq 2\sum_{i\in N} \|x_i(h_n)\|^2 + 2\sum_{i\in N} \|x_i(k)\|^2 \tag{3.37}$$

If $\sum_{i\in N} \|x_i(h_n)\|^2 \leq \sum_{i\in N} \|x_i(k)\|^2$ we have that $\sum_{i\in N} \|e_i(k)\|^2 \leq 4\sum_{i\in N} \|x_i(k)\|^2$. Otherwise, we have $\sum_{i\in N} \|e_i(k)\|^2 \leq 4\sum_{i\in N} \|x_i(h_n)\|^2$

Calling (3.30), we can conclude that

$$\Delta V(x(k)) \leq \sum_{j \in N} j_i \left\| e_i(k) \right\|^2 \tag{3.38}$$

Thus, for all $k \in H_n$ (active interval of DoS) If $\sum_{i \in N} \left\| x_i(h_n) \right\|^2 \leq \sum_{i \in N} \left\| x_i(k) \right\|^2$, the difference of the Lyapunov function rewritten as:

$$\begin{aligned} \Delta V(x(k)) &\leq \max\{j_i\} \sum_{j \in N} \left\| e_i(k) \right\|^2 \\ &\leq 4\max\{j_i\} \sum_{j \in N} \left\| x_i(k) \right\|^2 \\ &\leq \frac{4\max\{j_i\}}{\min\{\mu_i \lambda_{min}(P_i)\}} \sum_{j \in N} \mu_i V(x_i(k)) \\ &\triangleq \omega_2 V(x(k)) \end{aligned} \tag{3.39}$$

with $\omega_2 := \frac{4\max\{j_i\}}{\min\{\mu_i \lambda_{min}(P_i)\}}$. Also, $\forall k \in H_n$ with $\sum_{i \in N} \left\| x_i(h_n) \right\|^2 > \sum_{i \in N} \left\| x_i(k) \right\|^2$, one has

$$\Delta V(x(k)) \leq \omega_2 V(x(h_n)) \tag{3.40}$$

So, (3.39) and (3.40) implying that the Lyapunov function in the DoS attack's period H_n satisfy the following equation

$$V(x(k)) \leq (1 + \omega_2)^{k - h_n} V(x(h_n)) \tag{3.41}$$

During the transaction between stable and unstable modes.we will reflect the

the protocol waiting time, the Lyapunov function in this instant $V(x(k)) \leq (1-\omega_1)^{k-h_n-\tau_n-N\Delta}V(x(h_n+\tau_n+N\Delta))$ for $t \in [h_n+\tau_n+N\Delta, T_{n+1}[$ and $V(x(k)) \leq (1+\omega_2)^{k-h_n}V(x(h_n))$ for $t \in [h_n, h_n+\tau_n+N\Delta[$.

In conclusion, the overall behavior of the closed-loop system could be treated as a switching system with two modes. So, when simple iterations are applied to the Lyapunov function in and out of the presence of the DoS attacks status, we will get

$$V(x(k)) \leq (1-\omega_1)^{\left[k-\kappa_*-(\frac{1}{T}+\frac{\Delta_*}{\tau_D})k\right]}(1+\omega_2)^{\left[\kappa_*+(\frac{1}{T}+\frac{\Delta_*}{\tau_D})k\right]}V(x(0)) \tag{3.42}$$

To assure the stability of the last equation, (3.31) is obtained easily.

∎

Remark 14 *Theorem 3.1 offer a criterion to characterize the stability of distributed system in the form of (1.1) with an output feedback controller in the form of (3.1) and in the presence of DoS attack. The DoS attack is assumed to have constrained frequency and duration as described in Assumptions 5 and 6. The signals are exchanged over a communication channel with sampling interval Δ satisfying Assumption 7.*

Remark 15 *The stability of the MAIPS is affected by the sampling interval (Δ) of the Round-robin protocol since it delimits when the overall system is able to repair communication. In the case where the bounded duration and frequency DoS attack subjected to the MAIPS applying appropriate Round-robin inter-sampling time diminish the left-hand side of (3.31) that ensure the stability of the MAIPS. However, this is at the expense of high communication facilities.*

Table 3.1: Parameters of the Interconnected Power System

	Area (1)	Area (2)	Area (3)
T_t	0.65	0.4	0.3
T_g	0.2	0.1	0.1
D	0.7	0.9	0.9
H	12	10	8
R	0.05	0.0625	0.08

3.4 Simulation

A simulation result of three scenarios are shown in this section.The interconnected power system described in section (1.2) with the typology illustrated in 3.1 is tested with following parameters. The system parameters used in the simulation is listed in table 3.1. and the $N_12 = 2, N_13 = 2, N_23 = 4$ [74]. The controller gain as follows:

$$\begin{aligned} K_1 &= -4.072, K_2 = -0.453, K_3 = 0.951 \\ L_{12} &= -3.1422, \quad L_{13} = -0.0014 \\ L_{21} &= -1.34, \quad L_{23} = -2.76 \\ L_{31} &= -0.778, \quad L_{32} = 0.452 \end{aligned} \tag{3.43}$$

In the three scenarios a step load change (0.15 p.u.) is applied at time = 5s.

3.4.1 Nominal Situation

As shown in **Figure (3.2)** the MAIPS is stable in a normal situation with the controller gain in (3.43). The applied controller is able to return the deviation of the frequency to zero whenever the load fluctuates. In this case, the load change is occur-

ring at time 5s.

3.4.2 Under DoS Attack

In this scenario, a DoS attack was designed using Theorem 3.1 in section (3.2.1) and implemented on the system. **Figure 3.3** illustrate the series of the DoS attack which implemented on the interconnected system as shown the attack begins at time 6s. according to [75], the significant impact of the DoS attack is occurring when the attacker lunch the attacker during the load step change and before the Dynamic of LFC converges. In **Figure 3.3** the three interconnected power system is illustrated under the describer attack.

3.4.3 Stabilization under DoS

Using Lemma 3.1 and YALMIP,we found the follows:

$$P_1 = 10^{-11} \times \begin{bmatrix} 6.722 & 25.22 & -3.694 & 5049.80 \\ 25.23 & 3.706 & -18.225 & -4.661 \\ -3.694 & -18.225 & 4.49 & -11.734 \\ 5049.80 & -4.661 & -11.73 & 8.834 \end{bmatrix}$$

$$P_2 = 10^{-9} \times \begin{bmatrix} 4.616 & 38.95 & -2.258 & 52.194 \\ 38.95 & 2.658 & -22.674 & -3.0485 \\ -2.258 & -22.674 & 2.8964 & -233.71 \\ 52.194 & -3.0485 & -233.71 & 8.876 \end{bmatrix},$$

$$P_3 = 10^{-12} \times \begin{bmatrix} 4.4338 & 42.467 & -2.063 & 66.119 \\ 42.467 & 2.7692 & -20.318 & -2.7772 \\ -2.063 & -20.318 & 2.5825 & -441.62 \\ 66.119 & -2.778 & -4416.2 & 7.3978 \end{bmatrix},$$

$$Q_1 = 10^{-12} \times \begin{bmatrix} 78.083 & 1.6775 & 1.567 & 1.1737 \\ 1.6775 & 4.3809 & 3.2751 & 2.7048 \\ 1.5657 & 3.2751 & 3.1992 & 2.0830 \\ 1.1737 & 2.7048 & 2.0830 & 1.9653 \end{bmatrix},$$

$$Q_2 = 10^{-10} \times \begin{bmatrix} 1.2831 & 3.0258 & 2.5955 & 1.1653 \\ 3.0258 & 7.1397 & 6.1212 & 2.7491 \\ 2.5955 & 6.1212 & 5.2508 & 2.3568 \\ 1.1653 & 2.7491 & 2.3568 & 1.0593 \end{bmatrix},$$

$$Q_3 = 10^{-13} \times \begin{bmatrix} 93.998 & 2.6346 & 2.2218 & 1.1531 \\ 2.6346 & 7.4059 & 6.2284 & 3.2379 \\ 2.2218 & 6.2284 & 5.2496 & 2.7218 \\ 1.1531 & 3.2379 & 2.7218 & 1.4179 \end{bmatrix}$$

Then we obtain:

$$A = 10^{-10} \times \begin{bmatrix} 0.352 & 0.156 & 0.125 \\ 0.089 & 0.685 & 0.528 \\ 0.079 & 0.057 & 0.625 \end{bmatrix}$$

$$\Gamma = 10^{-8} \times \begin{bmatrix} 0.285 & 0.589 & 0.158 \\ 0.325 & 0.586 & 0.147 \\ 0.358 & 0.942 & 0.596 \end{bmatrix},$$

$$\Psi = 10^{-8} \times \begin{bmatrix} 0.258 & 0 & 0 \\ 0 & 0.354 & 0 \\ 0 & 0 & 0.425 \end{bmatrix}$$

Since the σ_1, σ_2 and σ_3 are (1.662), (1.541) and (1.284), respectively. the σ, in

this case, is chosen to be (1.2). Based on Assumption 3, we select the sampling interval $\Delta = 0.3$s. From this we calculate ω_1,ω_2 and ω_3 to be $(2.378(10)^4)$,and (1.631), respectively. As shown in **Figures 3.5**, the designing parameters able to maintain the stability of the MAIPS in the presence of the DoS attack and stable the frequency to the nominal state.

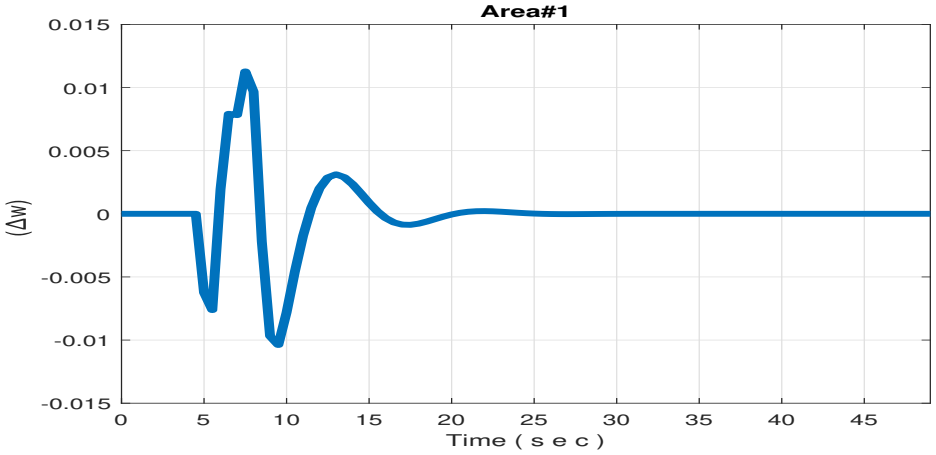

(a) Generator Area 1 with load change (0.15 p.u) at 5s

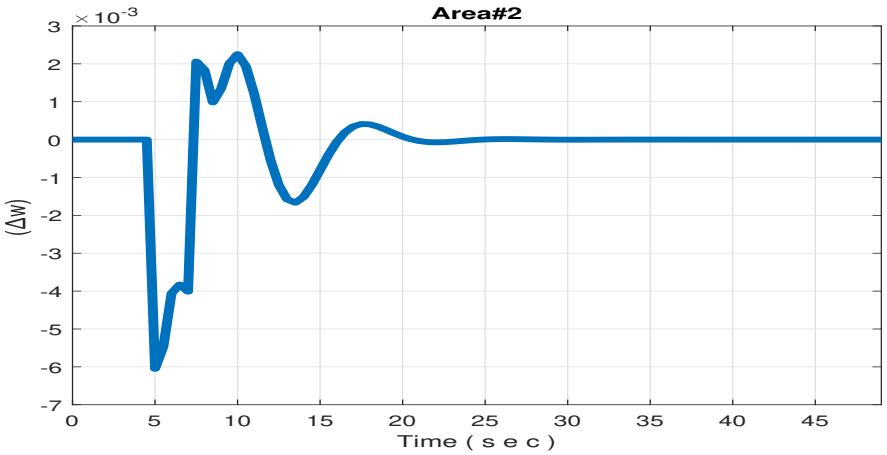

(b) Generator Area 2 with load change (0.15 p.u) at 5s

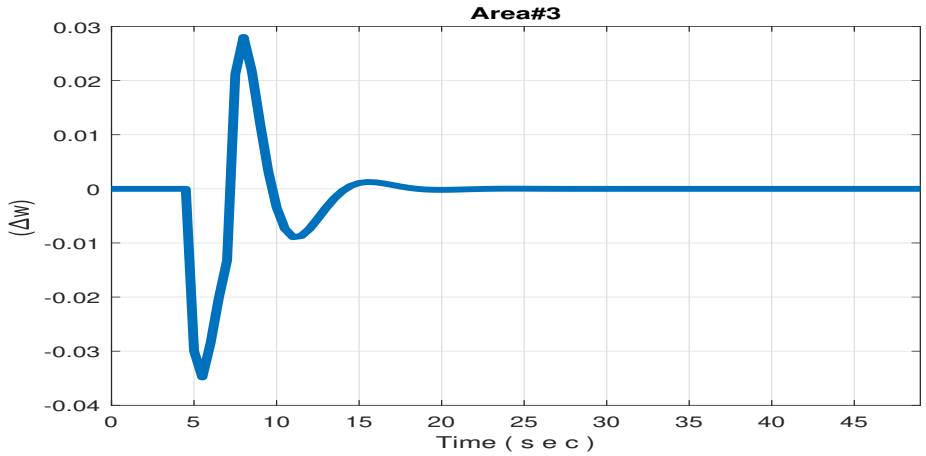

(c) Generator Area 3 with load change (0.15 p.u) at 5s

Figure 3.2: The output of the system in the nominal situation using the nominal T_s

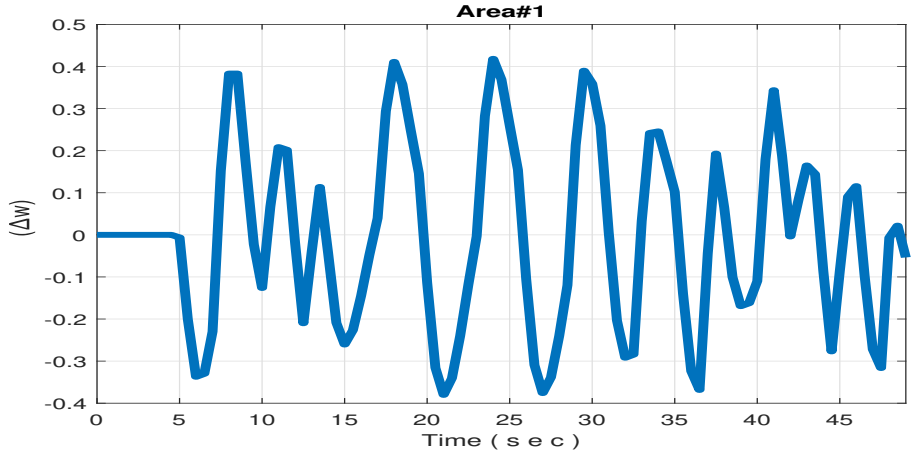

(a) Generator Area 1, load change (0.15 p.u) at 5s

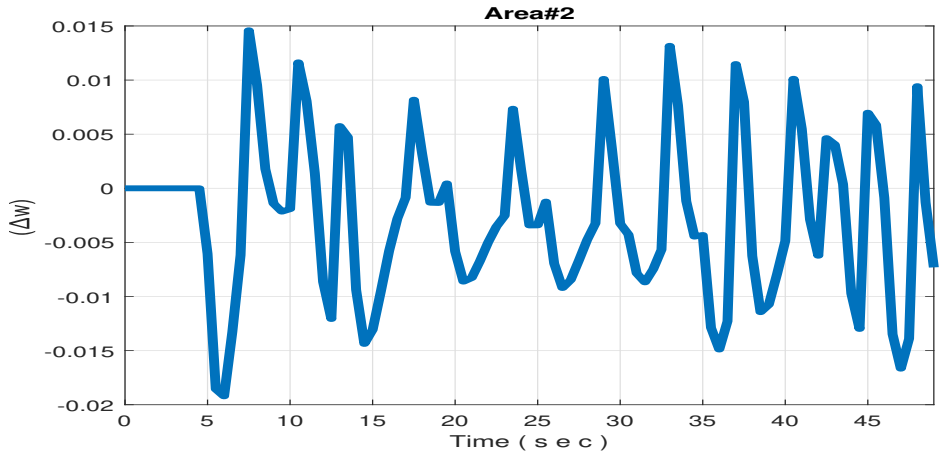

(b) Generator Area 2, load change (0.15 p.u) at 5s

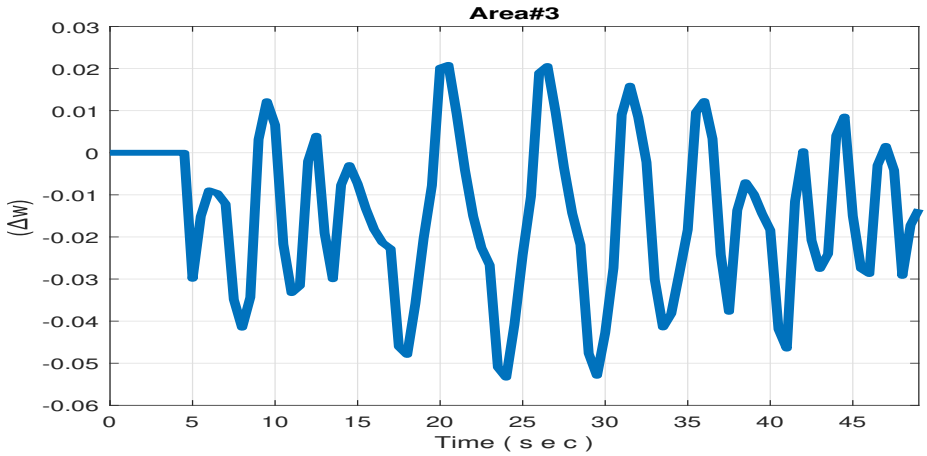

(c) Generator Area 3, load change (0.15 p.u) at 5s

Figure 3.3: The output of the system under DoS attacks using the nominal T_s

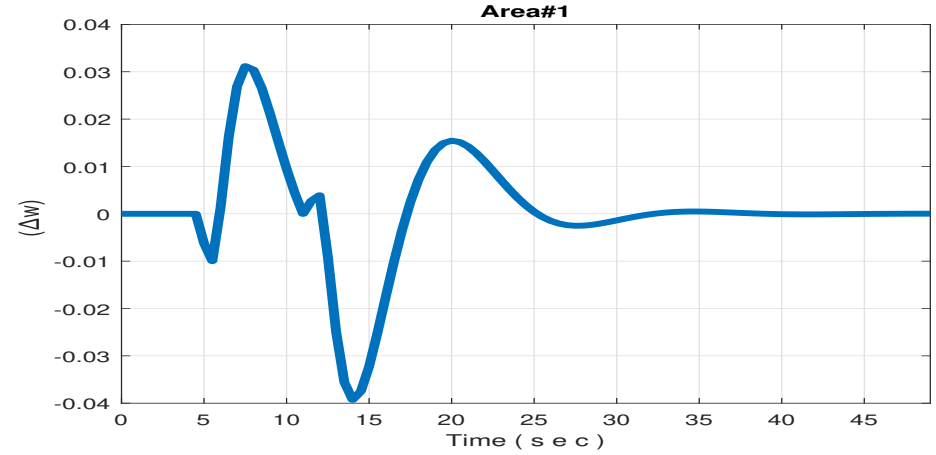

(a) Generator Area 1 , load change (0.15 p.u) at 5s

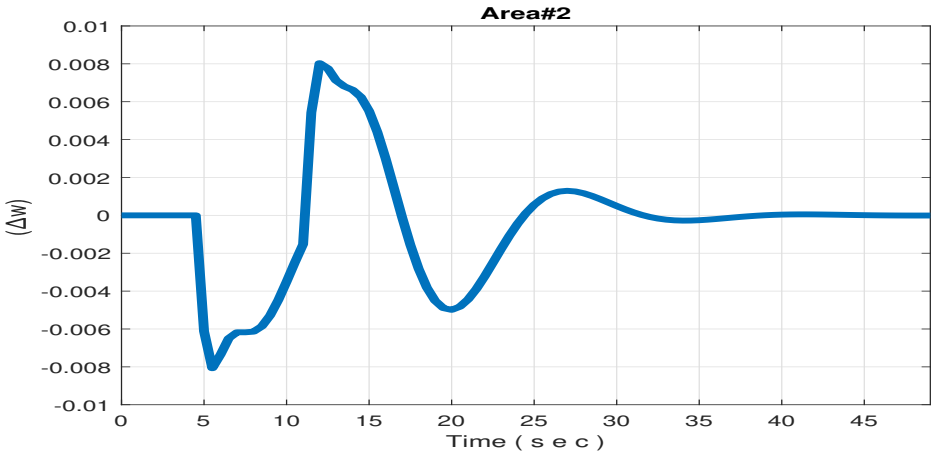

(b) Generator Area 2 , load change (0.15 p.u) at 5s

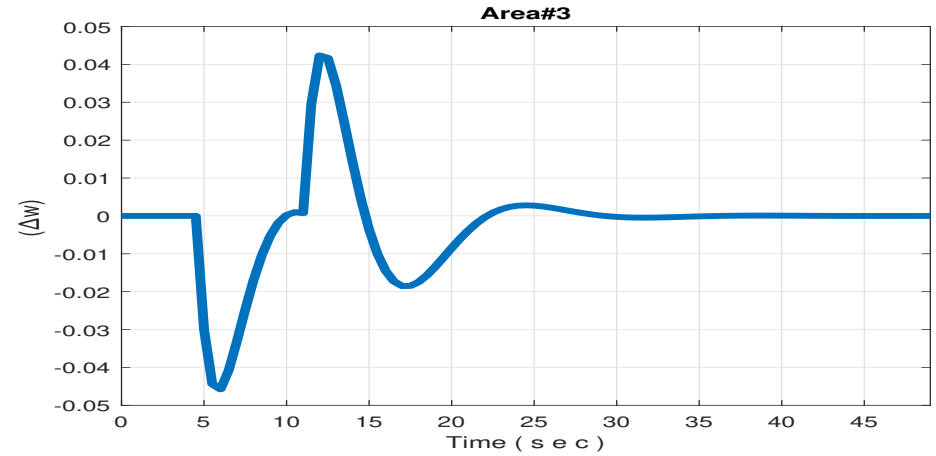

(c) Generator Area 3 , load change (0.15 p.u) at 5s

Figure 3.4: The output of the system in the nominal situation using the modified T_s

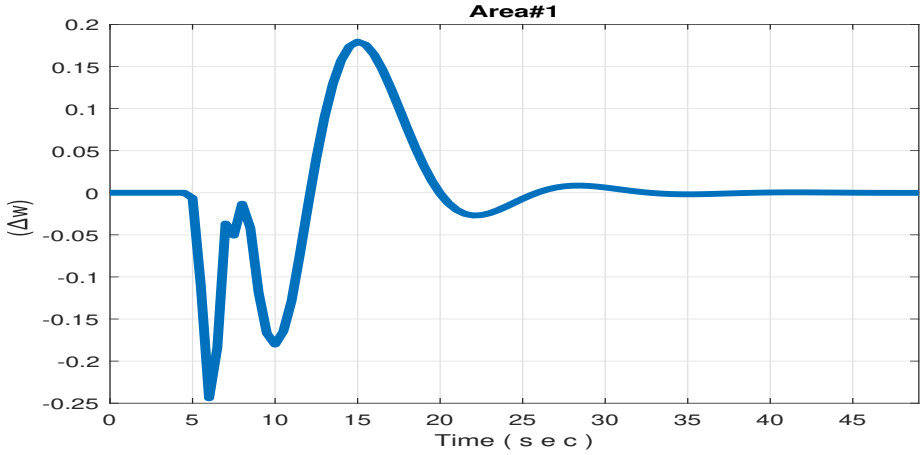

(a) Generator Area 1, load change (0.15 p.u) at 5s

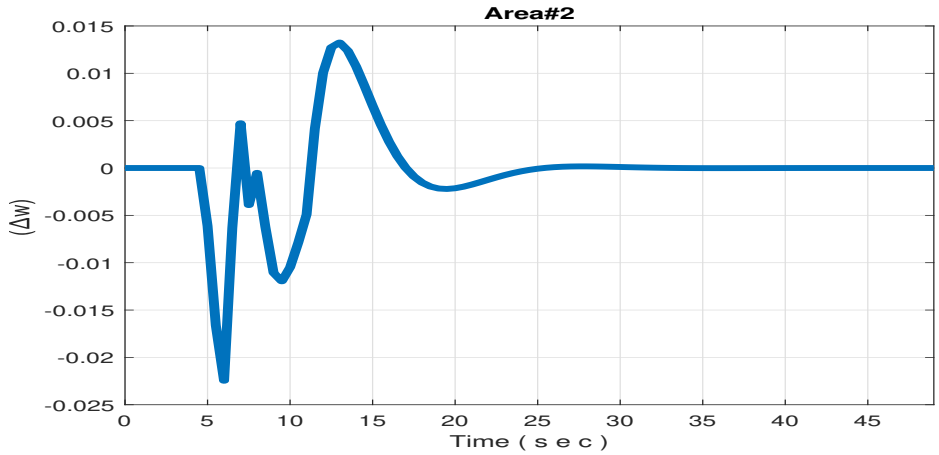

(b) Generator Area 2, load change (0.15 p.u) at 5s

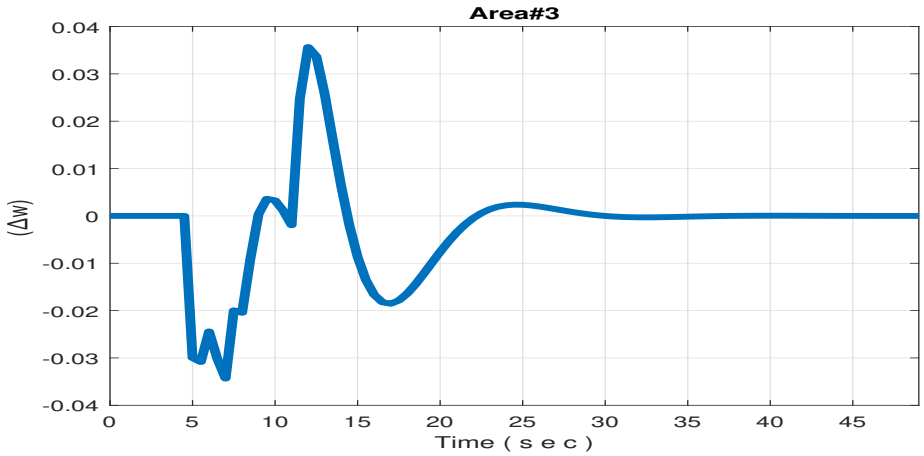

(c) Generator Area 3, load change (0.15 p.u) at 5s

Figure 3.5: The output of the system under DoS attacks using the modified T_s

CHAPTER 4

AN ONLINE ADAPTIVE AND MODEL PRODUCTIVE CONTROLLER

4.1 Introduction

The adaptive control method that resolving the considered Hamilton-Jacobi-Bellman equation for the optimal control challenges was presented in [62], [76]. In this way, the temporal difference equation is solved by the means of the value and policy iteration techniques to compute a sequence of control signals at which lead to the optimal control. According to [57], [77], the adaptive critics are perfect tools to realize the RL schemes, where two parted neural network assembly used to approximate the solution of the measured Bellman equation and the related optimal control sequence.

Looked at in this light, the following are the main contributions in this chapter:

- A discrete-time mathematical framework that employs a modified Bellman optimality equation is adapted to control the frequency of multi-area interconnected power system.

- A deep learning model is proposed to estimate the system states if the states dropped during the transmission with fulfillment packet loss probability.

- Online adaptive policy iteration based on the model-free control is developed to compensate the load frequency change for multi-areas interconnected power system in a distributed scheme with the present of the load variation.

- A model productive control scheme is addressed and compared with proposed online adaptive free-model controller. [78].In this work, we will use a two-level distributed structure and the performance was comped with the model productive (MPC) structure proposed in the [79]. The simulation results of three interconnected areas are given in section 4.4.

- Simulation of interconnected power system consist of three generation areas carried with applying the online adaptive policy iteration control and model productive control.

The remaining of the chapter was organized as follows: The modeling of a MAIPS was presented in Section 1.2. In Section 4.2, the framework and design of the adaptive controller was provided. Then, the model productive controller for a MAIPS was discussed in Section 4.3. Finally, the simulation of an illustrative example was presented in Section 4.4.

4.2 Adaptive Controller Design

The optimal control is driven here to find the optimal solution of the optimal control problem based on the Bellman optimally concepts [58]. For reliably, the packet loss due transmission delay or dropout during the transmission with packet loss probability p is modeled as a random process. This assumption is to model the behavior of the communication network. In this regard, the states measurements of the system are given as follows:

$$\bar{x}_i = \gamma(k)x_i(k) + (1-\gamma(k))\hat{x}_i(k) \tag{4.1}$$

Where $\gamma(k)$ is a Bernoulli random variable with $P_r(k=1) = 1-p$ with loss probability p. The estimated states $\hat{x}_i$ is obtained from the deep learning model explained in the coming section.

Definition 4.1 *A system in form (1.1) can be stabilized if there is a control input $u_i \in R^m$ which makes the system is asymptotically stable on a set of defined states.*

Remark 16 *Since the states are grouped from the distributed subsystem and transmitted to the controllers together as network packets. This transmission of the packet through the communication network may cause a non-simultaneous arrival of the packets. The packet loss is due to many reasons, for instance, the occurrence of communication failures or message collisions. The packet loss is simulated by the variable $\gamma(k)$. However, to deal with the packet loss issue, we propose a deep learning model to estimate the states of the subsystem.*

4.2.1 Deep Learning States Estimator

The deep long short term memory (LSTM) model is proposed in this work to estimate the states of each subsystem. The model is trained on the data-set collected and tested on the unseen data-set to validate the performance of the proposed model. The mathematical model of the LSTM is given as

$$\begin{aligned}
\hat{x}_i(k) &= H_i(k)tanh(S_i(k)) \\
H_i(K) &= \sigma(W_h Z + b_h) \\
S_i(k) &= F_i(k)S_i(k-1) + I_i(k)\tilde{S_i(k)} \\
\tilde{S_i(k)} &= tanh(W_S Z + b_S) \\
I_i(k) &= \sigma(W_I Z + b_I) \\
F_i(k) &= \sigma(W_F Z + b_F)
\end{aligned} \tag{4.2}$$

Where $Z = [\hat{x}_i(k-1), x_i(k-1), \ldots, x_i(k-w)]$, w is the window size of the model. σ is a sigmoid function. $F_i(k)$,$I_i(k)$, and $S_i(k)$ is an output of the forget gate layer, the output of the input gate layer, and the cell state, respectively. $W_H b_H$,$W_S b_S$,$W_I b_I$, and $W_F b_F$ are the output, cell state, input gate, and forget gate wights and bias, respectively. **Figure 4.1**, illustrate the observed states verse the system states estimated using the proposed LSTM model with the stem plot of the mean square error of each estimation.

Remark 17 *It is worth noting that the proposed deep learning model used is a long short term memory (LSTM) with* 0.3 *dropout layer. The model is trained by*

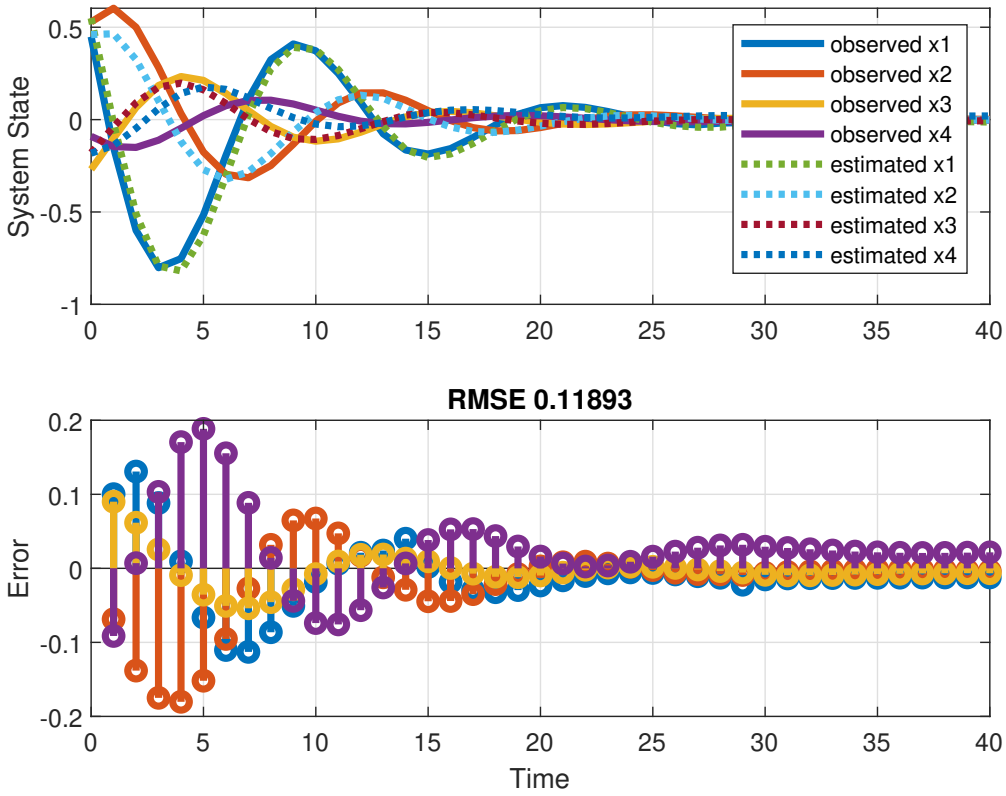

Figure 4.1: Estimated states vs. Observed states

the collected dataset that generated from the model. An input and load variation was generated by a random Gaussian signal while the time when the load variation happened was changed arbitrarily. The proposed deep estimator is tested on the unseen dataset as shown in the ***Figure 4.1****. The proposed LSTM model is performing well and able to approximate the dynamic behave of the system with maximum root mean square error (RMSR)* 0.11893.

The optimal value function is the Bellman optimally [58] and adapted to load frequency control problem. Assuming the model is stabilizable on some sets, and we

can find the optimal control u_i such that

$$u = -R^{-1}B^T \frac{\partial V(\bar{x}_{i+1}, u_{i+1})}{\partial t} \bar{x}_i \tag{4.3}$$

Where V is following the modified Bellman equation proposed in [80]. The optimal Bellman equation, in this case, is considering both the states of the model as well as the control input. So the optimal Bellman equation is defined such that

$$V(\bar{x}_i, u_i) = \frac{1}{2}(\bar{x}_i^T S \bar{x}_i + u_i^T R u_i) + V(\bar{x}_{i+1}, u_{i+1}) \tag{4.4}$$

Solving (4.4) for the optimal control input u_i we lead to

$$u^\circ = -R^{-1}B^T \frac{\partial \tilde{V}^\circ(\bar{x}_{i+1}, u_{i+1})}{\partial t} \bar{x}_i \tag{4.5}$$

From (4.5) and (4.4) the optimal Bellman equation is given as

$$V^\circ(\bar{x}_i, u_i^\circ) = \frac{1}{2}(\bar{x}_i^T S \bar{x}_i + u_i^{\circ T} R u_i^\circ) + V^\circ(\bar{x}_{i+1}, u_{i+1}^\circ) \tag{4.6}$$

The optimal control (4.5) is induced to solve the modified Bellman equation (4.6). The main objective of this work is to design a robust control that has the ability to stabilize the system dynamic. The promising approach is to use an online model-free control iteration that proposed in this brief. This approach will be applied to the power system and examine the effective of this approach in distributed system.

The main difficulty of this optimal method is that the accuracy of the method

depends on the knowledge of the system, and it requires a deep knowledge of the dynamic of the controlled system. For this reason, an improved control structure is proposed in this chapter to overcome these challenges. The promising approach as shown in literature is the policy iteration techniques. This control structure is overcome many classical controllers including the model productive control as we will compare the performance of the online adaptive control with the MPC in the simulation section. In the following section, we develop an online adaptive structure and adjusted it to be used in the power interconnected system.

4.2.2 Online Adaptive Policy Iteration

In this work, a value function $Q(\bar{x}_i, u_i)$ have been considered. Let the Q to be defined such that

$$Q(\bar{x}_i, u_i) = \frac{1}{2}(X_i^T P X_i) \tag{4.7}$$

Where $X_i = [\bar{x}_i^T; u_i^T]$ a column vector that compile the states of the system and the control signals. P is a square positive definite Routh Horowitz matrix of proper nxn dimension. P is structured as following

$$P = \begin{bmatrix} P_{XX} & P_{Xu} \\ P_{uX} & P_{uu} \end{bmatrix} \tag{4.8}$$

Approximating the function $F(\bar{x}_i, u_i)$ by the $Q(\bar{x}_i, u_I)$ such that

$$\tilde{V}(\bar{x}_i, u_i) = \sum C(\bar{x}_i, u_i) \simeq Q(\bar{x}_i, u_i) \tag{4.9}$$

From (4.9) we can solve for the optimal control input u° which written as

$$u^\circ = min(Q(\bar{x}_i, u_i) = -P_{uu}^{-1} P_{uX} \bar{x}_i \tag{4.10}$$

Here P is An invertible matrix because it is a positive definite matrix as defined above which ensure the existence of the optimal control input u°. In this manner, we can rewrite the approximated Bellman equation (4.9) such that

$$Q(\bar{x}_i, u_i) = \frac{1}{2}(\bar{x}_i^T S \bar{x}_i + u_i^T R u_i) + Q(\bar{x}_{i+1}, u_{i+1}) \tag{4.11}$$

The main stone of the proposed model free policy iteration is the complement between the optimal value function (4.6), the optimal control (4.10) and the $Q(\bar{x}_i, u_i)$ in (4.11). The connection between these three equations will lead to obtain the optimal control signal u° as defined in (4.10) which present a solution for the modified Bellman equation. Considering the value function with the optimal policy u°, the value function is written as

$$Q(\bar{x}_i, u_i^\circ) = \frac{1}{2}(\bar{x}_i^T S \bar{x}_i + u_i^{\circ T} R u_i^\circ) + Q(\bar{x}_{i+1}, u_{i+1}^\circ) \tag{4.12}$$

The proof of convergence of the proposed adaptive policy iteration is given in proof

4.2.2 after discussing the implementation and the procedure of the proposed method.

Remark 18 *The main challenge of the model-free online control iteration is that there is no existing method to compute the value function Q as illustrated in equation* (4.12)*. Besides, no possible way to calculate the matrix M. This leads us to utilizes the talented approximation method which an actor-critic neural network technique. In this manner, two neural networks are used. The actor policy approximation neural network is used to estimate the optimal control signal u while the critic neural network is used to approximate the value function [57]. The combined actor-critic neural network is adjusted and repeated in a described procedure such that the weights of each neural network converge.*

In this regard, the estimated value function can be computed as

$$\hat{Q}(\bar{x}_i, \hat{u}_i) = \frac{1}{2}(\hat{X}_i^T C_w \hat{X}_i) \tag{4.13}$$

Where $C_w \in R^{(m+n)x(m+n)}$ is a symmetric positive definite matrix which will be presented as critic neural network wights. $\hat{X}_i^T = [\bar{x}_i^T, \hat{u}_i^T]$. The equation (4.13) is adjusted to be implemented in a single layer network such as

$$\hat{Q}(\bar{x}_i, \hat{u}_i) = \frac{1}{2}\tilde{X}_i^T C_w \tilde{X}_i = vec(C_w)^T(\hat{X}_i \otimes \hat{X}_i) \tag{4.14}$$

Where $\hat{C}_w = vec(C_i)$ and $\otimes$ is representing Kronecker product $\hat{X}_i = \hat{X}_i \otimes \hat{X}_i$. In this case, the $vec(.)$ is an operation which take the C_w symmetric matrix and reshape

it to a vector. This operation is considering only the upper or lower triangular matrix. This is the reason why in the implementation the wights are updated each $\frac{(n+m)^2(n+m)}{2}$. The vector $\hat{X}_i$ is a quadratic polynomial that containing all possible products of X_i.

To update the critic neural network weights, we consider the following mapping equation. Where the $Q_i^desired = F(\bar{x}_i, u_i)$ is mapped to the $(\tilde{X}_i - \tilde{X}_{i+1})$

$$\tilde{W}_c^T(\tilde{X}_i - \tilde{X}_i + 1) = \hat{Q}_i^{desired} = \frac{1}{2}(\bar{x}_i^T S \bar{x}_i + \hat{u}_i^T R \hat{u}_i) \tag{4.15}$$

Where the $\tilde{X}_i^T = [\hat{X}_1^1 \hat{X}_2^1 \ldots, \hat{X}_1^2 \hat{X}_2^2 \ldots, \hat{X}_1^3 \hat{X}_2^3 \ldots]$ in the range $k = 1, 2, \ldots, \frac{(n+m)^2(n+m)}{2}$, this term is produced by the operation $(\hat{X}_i \otimes \hat{X}_i)$. Then updating process will be done after collecting $\frac{(m+n)(m+n+1)}{2}$ data point using (4.15). The goal of critic neural network is to minimize the error defined as following.

$$Err_c = \|\tilde{C}_w \upsilon_m - \upsilon_y\|^2 \tag{4.16}$$

Where υ_m is a matrix with correct diminution whose column in include $(\tilde{X}_i - \tilde{X}_{i+1}$ and υ_y is a row vector composed of $Q_i^{desired}$. In this work, the gradient decent is applied to minimize the error so the wight update rule is expressed as

$$(\tilde{C}_w(i+1))^T = (\tilde{C}_w(i))^T - l(\tilde{C}_w \upsilon_m - \upsilon_y).(\upsilon_m)^T \tag{4.17}$$

Where l is the critic network learning rate, and bounded by 0 and $1, (0 < l < 1)$.

While the online critic network is running and, in each time step i, the actor neural network estimating the state vector $\bar{x}_i$ by mapping the optimal control policy $\hat{u}_i$ using the following linear equation.

$$\hat{u}_i = A_w^T \bar{x}_i \tag{4.18}$$

Where the actor wights are presented by the $A_w \in R^{nxm}$. In the actor neural network, the goal is to compute the desired $\hat{u}_i$ using the critic weight matrix as following.

$$\hat{u}_i^{desired} = -C_{\hat{u}\hat{u}}^{-1} C_{\hat{u}x} \bar{x}_i \tag{4.19}$$

The critic weight matrix C_w is defined as follows

$$C_w = \begin{bmatrix} C_{xx} & C_{x\hat{u}} \\ C_{\hat{u}x} & C_{\hat{u}\hat{u}} \end{bmatrix} \tag{4.20}$$

Where $C_{xx} \in R^{nxn}$ and $C_{\hat{u}\hat{u}\in R^{mxm}}$ are square matrices.

The same as critic the actor neural network use the gradient descent method to update the weights of the actor neural network as following

$$\tilde{A}_w^T(i+1) = (\tilde{A}_w(i))^T - l(\hat{u}_i - \hat{u}_i^{desired})\bar{x}_i^T \tag{4.21}$$

l is the actor neural network learning rate.

Algorithm 1 Online Adaptive Policy Iteration with Actor-critic Neural Network

Require: Optimal control policy.
Ensure: $u^\circ = min\{Q(\bar{x}_i, u_i)\}$
1: $i = 0$ time index. ▷ Initialization.
2: Setting the Stopping Condition err err and ϵ.
3: l Setting the Learning rate.
4: Initialize the C_w.
5: Initialize the A_w.
6: **while** $err > \epsilon$ **do**
7: **for** subsystem $i \in m$ **do**
8: Calculate the control input $\hat{u}_i$ and desired control input using (4.18) and (4.19)
9: Calculate the control input $\hat{u}_{i+1}$ using (4.18)
10: Compute the $\hat{Q}_i$ and $\hat{Q}_{i+1}$ using (4.14)
11: Compute the $\hat{Q}_i^desired$ using (4.15)
12: **if** $i + 1 == \frac{(n+m)^2(n+m)}{2}$ **then**
13: Update the C_w using (4.17).
14: Update the A_w using (4.21).
15: **end if**
16: $i = i + 1$ ▷ update index
17: **end for**
18: $j = j + 1$
19: **end while**

Algorithm 1 summarize the implementation procedure of actor-critic neural network where the value function and desired optimal control policy are estimated. The main advantage of this algorithm is that the actor-critic neural network is performing the approximation process in real-time with no need for the dynamic model. The mathematical model discussed above just use to generate a simulation and to take the measurements values. In real work, the proposed method can be connected directly

to any such system.

In this part, we will express the proof of **Algorithm 1** convergence. We need in this part to show two main points.

Theorem 4.1 *If **Algorithm 1** is applied to the system described by* (1.1) *with derived valued function in* (4.11) *and control input in* (4.10) *starting with utilizable control input* u_0*. Then*

1. *The generated series of control signal* u_i *stabilizing the system* (1.1)*.*
2. *The generated value functions are monotonously decreasing meaning* $Q_1 \geq Q_2 \geq Q_3 \geq Q_i$*.*

Proof. Starting from equation (4.11) We regarded the $Q(\bar{x}_i, u_i)$ as a Lyapunov function with input $u_i, \forall i$. Then

$$Q(\bar{x}_{i+1}, u_{i+1}) - Q(\bar{x}_i, u_i) = \triangle C(u_i, u_{i+1}) \leq 0, \forall i \tag{4.22}$$

evaluation the $\triangle C(u_i, u_{i+1})$

$$\begin{aligned} \triangle C(u_i, u_{i+1}) &= \sum \frac{1}{2}(u_i - u_{i+1})^T R(u_i - u_{i+1}) \\ &\quad + u_{i+1}^T R(u_i - u_{i+1}) \end{aligned} \tag{4.23}$$

From this we prove that $\triangle C(u_i, u_{i+1}) \geq 0$, $\forall i$ which means that $\triangle C(u_i, u_{i+1}) \geq$

$Q(\bar{x}_{i+1}, u_{i+1})$ meaning that the u_{i+1} stabilizing the system. Noting that the u_0 most be a stabilized control input.

Now, to prove that the generated value functions are monotonously decreasing meaning we have to prove that $Q_1 \geq Q_2 \geq Q_3 \geq Q_i$.

From (4.22)

$$Q(\bar{x}_{i+1}, u_{i+1}) - Q(\bar{x}_i, u_i) \leq -\triangle C(u_i, u_{i+1}) \leq 0 \tag{4.24}$$

$$Q(\bar{x}_{i+1}, u_{i+1}) - Q(\bar{x}_i, u_i) + \triangle C(u_i, u_{i+1}) = 0 \tag{4.25}$$

hence,

$$\begin{aligned} 0 &\leq Q(\bar{x}_{i+1}, u_{i+1}) - Q(\bar{x}_i, u_i) \\ &\leq Q(\bar{x}_{i+2}, u_{i+2}) - Q(\bar{x}_{i+1}, u_{i+1}) \end{aligned} \tag{4.26}$$

Applying the summation to both sides of ((4.26))

$$\begin{aligned} 0 &\leq \sum_{i=k}^{\infty} Q(\bar{x}_{i+1}, u_{i+1}) - Q(\bar{x}_i, u_i) \\ &\leq \sum_{i=k}^{\infty} Q(\bar{x}_{i+2}, u_{i+2}) - Q(\bar{x}_{i+1}, u_{i+1}) \end{aligned} \tag{4.27}$$

as a result

$0 \leq Q_i(\bar{x}_\infty, u_\infty) - Q_i(\bar{x}_k, u_k) \leq Q_{i+1}(\bar{x}_\infty, u_\infty) - Q_{i+1}(\bar{x}_k, u_k)$

By utilizing the proof 1 the $Q_i(\bar{x}_\infty, u_\infty) - Q_i(\bar{x}_k, u_k)$ will be always negative that means

$Q_i(\bar{x}_{k+1}, u_{k+1}) \geq Q_i(\bar{x}_k, u_k) \geq 0$ from this we can prove that

$Q_1 \geq Q_2 \geq Q_3 \geq Q_i$.

By this mean, we have proof that **Algorithm 1** is generating a series of control input signals u_i with monotonically decreasing value functions Q_i this value function is bounded by $Q^0 and 0$. This implying that the value function generated by **Algorithm 1** converges to its optimal value. ∎

4.3 Model Predictive Controller

In this section, a distributed model predictive controller (DMPC) is addressed and implemented on the simulation section. The MPC designed for the LFC of multi-area interconnected power system. Considering the system described in (1.1) in section II. and assuming that the matrix pair (A_i, B_i) is controllable for all subsystems.

To design the MPC for the system (1.1) that guarantee the asymptotic stability of the system. We will consider the system in (1.1). Our goal is to relate inputs it to $u_i(k)$.

In this manner, for each subsystem in the MAIPS, the optimal control problem at instant k is formulated in the following objective function:

$$\mathscr{C} = min_{u_i(.)} \sum_{k=0}^{\mathscr{N}-1} x_i(k)^T Q x_i(k) + u_i(k)^T R u_i(k) \tag{4.28a}$$

s.t.

$$\begin{aligned}
\bar{x}_i(k+1) &= A_{ii}\bar{x}_i(k) + B_i\bar{u}_i(k) && (4.28b)\\
&\quad + E_i\bar{f}_i(k) + \sum_{i\in N} A_{ij}\bar{x}_{ij} \\
\bar{x}_i(k; x_i(k), k) &= x_i(k) && (4.28c)\\
|(x_{i2}(k) - x_{i3})/T_{CH_i}| &\leq 0.0012 && (4.28d)\\
\bar{u}_i(k) &\leq \frac{1}{2} && (4.28e)
\end{aligned}$$

where $Q \in \mathcal{R}^{n\times n}$ and $R \in \mathcal{R}^{m\times m}$ denote positive definite and symmetric weighting matrices. $\mathscr{N}$ is the prediction horizon, $\mathscr{C}$ is the cost function. The actual measured system states is used in the MPC controller to predict the future states within the time horizon $\mathscr{N}$.

There are several methods address solving such problem, In this work, we extend the method used in [81] to be used in the discrete system. The implantation of the MPC controller is summarized in **Algorithm 2**. Assuming that the state of the i-the area $x_i(k)$, states of the interconnected areas $x_j(k)$, and the load deviation $f_i(k)$ can be obtained or estimated directly in each controller.

Remark 19 *By implementing MPC scheme, it is not necessary for every controller to communicate with every other controller. Controller i only needs to communicate with coupled controller j. If the system is loosely coupled, the amount of communication will be reduced.*

Algorithm 2 Distributed model predictive controller

For the $i-th$ area controller, the distributed model predictive algorithm described in the following steps:
Step 1 Receive the states of the connected areas $x_i(k)$, and the measurements of $x_i(k)$ and $f_i(k)$;
Step 2 At sampling time k, set the states $\bar{x}_i(k) = x_i(k)$, $\bar{x}_j(k) = x_j(k)$ and $\bar{f}_i(k) = f_i(k)$;
Step 3 Solve the optimal problem described in (4.3);
if *Step 3* is feasible **then**
    $u_i(k) = \bar{u}_i(k)$;
end if
if *Step 3* is not feasible **then**
    $u_i(k) = \bar{u}_i(k-1)$;
end if
Applying the control signal $u_i(k)$, set $k = k+1$ and return to *Step 1* at the next sample time;

4.4 Simulation and Results

In this section, we implemented the proposed Online Adaptive Policy iteration algorithm and MPC on the MAIPS described in section 4.2. The three areas model parameters utilized on this work is tabled in table 2.1

We carry on the simulation using MATLAB to test the performance of the developed algorithms in this work on the three interconnected power systems. The structure of the coupled areas and the distributed control used in this work is illustrated in **Figure 1.2**. The performance of the system is examined where the interconnected power system is subjected to the different loads applied to each generation area at different time (at 5 sec, 8 sec).

The performance of the proposed adaptive algorithm is compared with the MPC as shown. In **FIGURE 4.2** the ACE of the three areas is illustrated. In **Figure 4.3** the trajectory states $x_1(k)$ and $x_4(k)$ of area-1 are shown where $x_1(k)$ and $x_4(k)$ represent

the frequency deviation and the deviation of power flow of the tie-line, respectively. In the same manure, area-2 states trajectories are presented in **Figure 4.4**, and states trajectories of the states of area-3 are presented in **Figure 4.5**.

Remark 20 *The main advantage of the adaptive controller proposed in this brief is the model-free scheme which is preferred in the case of uncertainty of load variation and adapts to the uncertainty through multiple trials of the actor and critic networks. However, our results demonstrate that, with a proper formulation of the optimal control, it is possible to obtain similar results for the adaptive policy iteration and MPC. Additionally, The adaptive methods successfully avoid constraint violations and substantially reduce regret compared to MPC.*

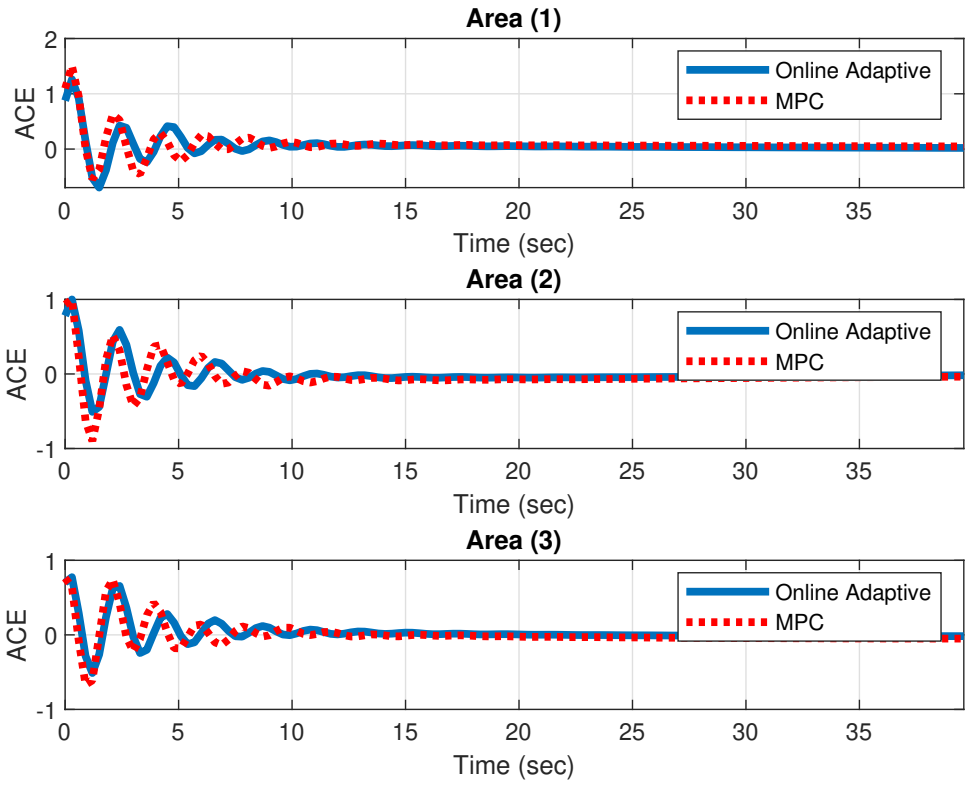

Figure 4.2: Area Control Error (ACE)

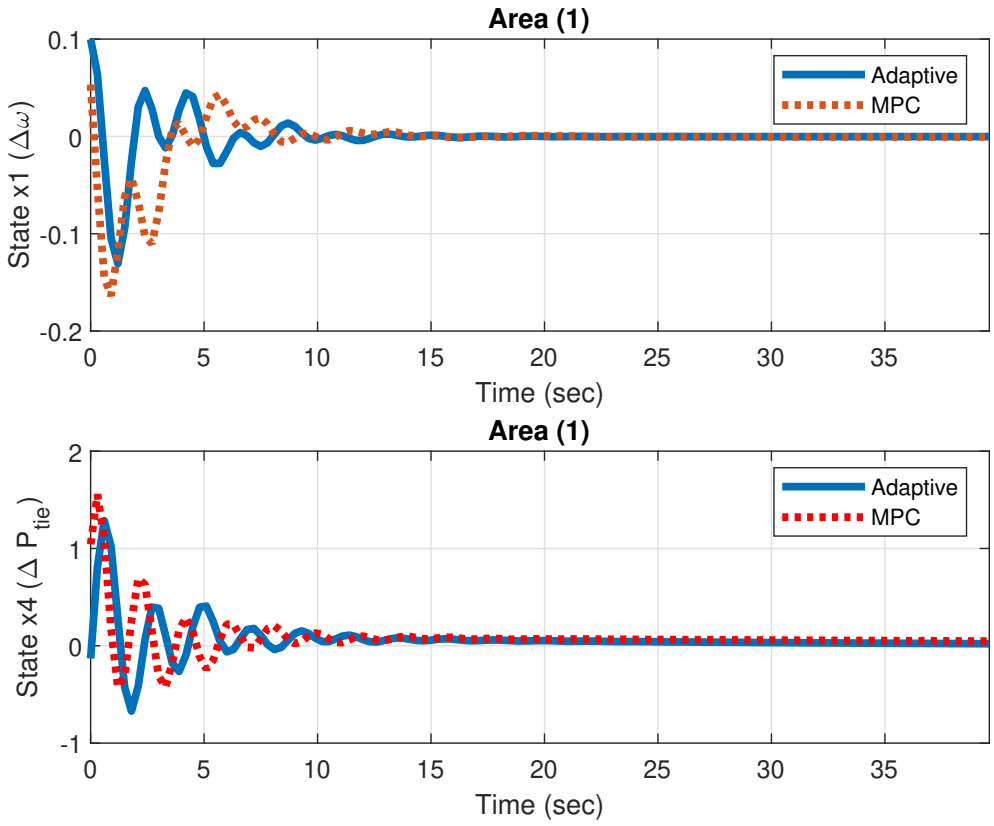

Figure 4.3: States trajectory of $area(1)$.

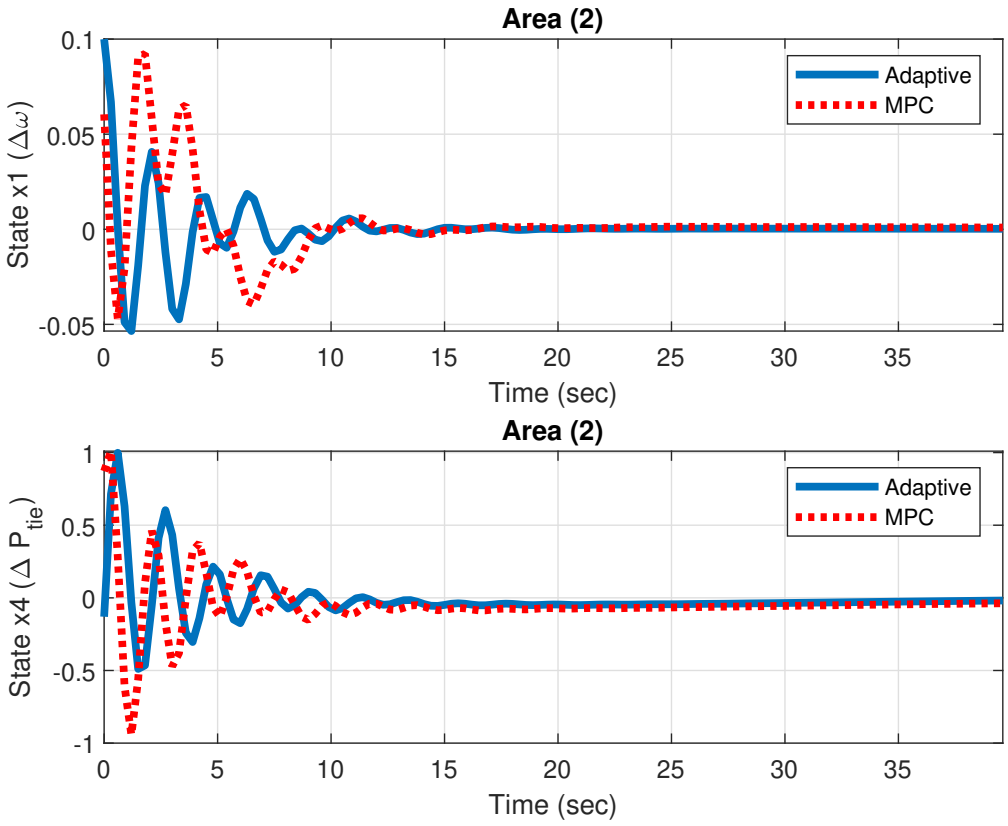

Figure 4.4: States trajectory of $area(2)$.

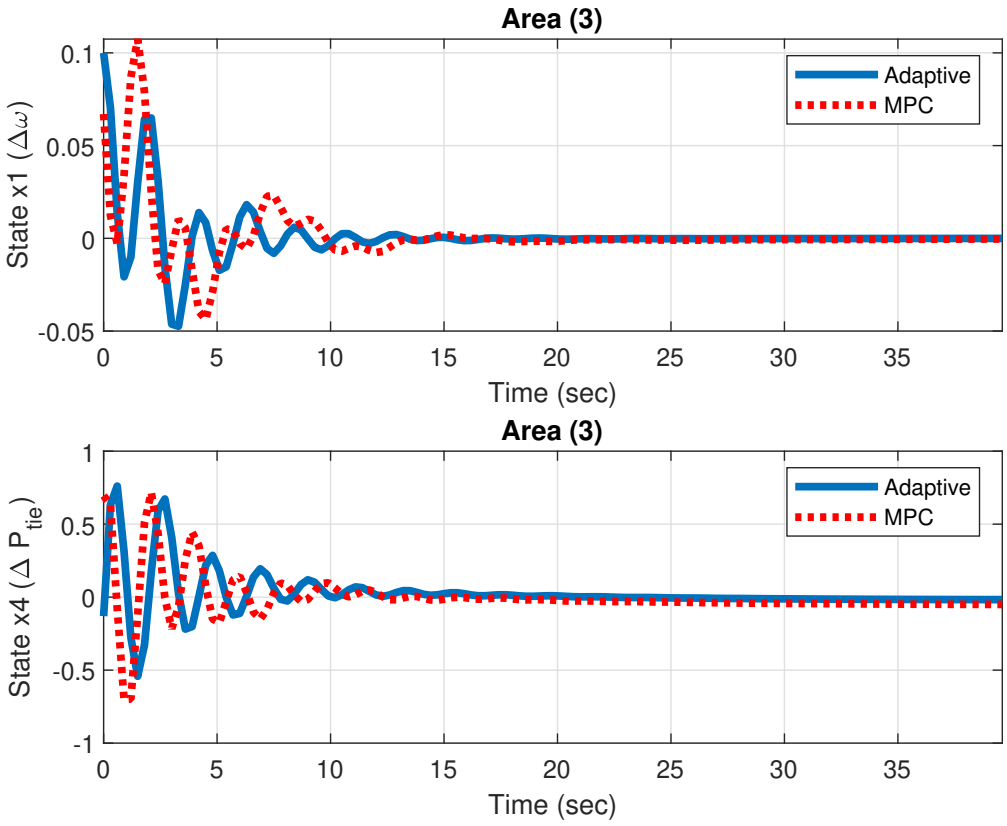

Figure 4.5: States trajectory of $area(3)$.

CHAPTER 5

CONCLUSION AND FUTURE WORK

With the continuous increase of the electricity demand, power systems are more essential for the modern lifestyle. Recently, power generation areas have been connected to meet the demand load which considered as large scale NCS. This system provide customers with the required electricity such that if one generation area fails, others con cover the demand. Power systems are vulnerable to cyber-attacks and transmission delay which can affect the stability of the system and cause failure. In this work, we explore the stabilization of a class of NCS such as a multi-area interconnected power system (MAIPS) in the presence time delay and denial of service (DoS) attack that prevents the exchange of data over the communication channel. First, a static feedback controller is applied to stabilize the MAIPS in the nominal situation. Then, the stability of the MAIPS is characterised when the system is subjected to the communication time delay and DoS attack while considering predetermined limits of the

duration and the frequency of delay.

Furthermore, The online adaptive policy iteration has been proposed to control the load frequency on the power system. It has been tested in the three interconnected power generation areas. The result shows the performance of the proposed controller and its ability to stabilize the system. The variation on the active load is reflected in the system and the proposed control performs well to regulate the frequency to the nominal values. The proposed adaptive policy iteration controller is compared with the MPC while the main advantage of the proposed scheme does not rely on the model dynamic of power systems. Finally, an illustrative example of three area interconnected power system with several scenarios are presented to verify the effectiveness of the proposed methods.However, We believe that a hybrid control technique that combing the adaptive model free and MPC is a promising future research interest, and we hope to extend our work in the future to include such hybrid methods. In addition, a controller base on data-driven is a promising control direction in this field.

REFERENCES

[1] P. Kundur, "Power system stability," *Power system stability and control*, pp. 7–1, 2007.

[2] Y. Wang, R. Zhou, and C. Wen, "Robust load-frequency controller design for power systems," in *IEE proceedings C (generation, transmission and distribution)*, vol. 140, no. 1. IET, 1993, pp. 11–16.

[3] H. Bevrani, *Robust power system frequency control*. Springer, 2009, vol. 85.

[4] H. Shayeghi, H. Shayanfar, and A. Jalili, "Load frequency control strategies: A state-of-the-art survey for the researcher," *Energy Conversion and management*, vol. 50, no. 2, pp. 344–353, 2009.

[5] M. Ma, X. Liu, and C. Zhang, "Lfc for multi-area interconnected power system concerning wind turbines based on dmpc," *IET Generation, Transmission & Distribution*, vol. 11, no. 10, pp. 2689–2696, 2017.

[6] J. Alipoor, Y. Miura, and T. Ise, "Power system stabilization using virtual synchronous generator with alternating moment of inertia," *IEEE journal of Emerging and selected topics in power electronics*, vol. 3, no. 2, pp. 451–458, 2014.

[7] L. M. Castro and E. Acha, "On the provision of frequency regulation in low inertia ac grids using hvdc systems," *IEEE Transactions on Smart Grid*, vol. 7, no. 6, pp. 2680–2690, 2015.

[8] W. Zhang, K. Rouzbehi, A. Luna, G. B. Gharehpetian, and P. Rodriguez, "Multi-terminal hvdc grids with inertia mimicry capability," *IET Renewable Power Generation*, vol. 10, no. 6, pp. 752–760, 2016.

[9] S. Sridhar, A. Hahn, and M. Govindarasu, "Cyber–physical system security for the electric power grid," *Proceedings of the IEEE*, vol. 100, no. 1, pp. 210–224, 2011.

[10] M. Vrakopoulou, P. M. Esfahani, K. Margellos, J. Lygeros, and G. Andersson, "Cyber-attacks in the automatic generation control," in *Cyber Physical Systems Approach to Smart Electric Power Grid*. Springer, 2015, pp. 303–328.

[11] M. Khalaf, A. Youssef, and E. El-Saadany, "Joint detection and mitigation of false data injection attacks in agc systems," *IEEE Transactions on Smart Grid*, vol. 10, no. 5, pp. 4985–4995, 2018.

[12] D. Ding, Q.-L. Han, Y. Xiang, X. Ge, and X.-M. Zhang, "A survey on security control and attack detection for industrial cyber-physical systems," *Neurocomputing*, vol. 275, pp. 1674–1683, 2018.

[13] Y. Zhang and T. Yang, "Decentralized switching control strategy for load frequency control in multi-area power systems with time delay and packet losses," *IEEE Access*, vol. 8, pp. 15 838–15 850, 2020.

[14] K. Pan, P. Palensky, and P. M. Esfahani, "From static to dynamic anomaly detection with application to power system cyber security," *IEEE Transactions on Power Systems*, vol. 35, no. 2, pp. 1584–1596, 2019.

[15] C.-W. Ten, C.-C. Liu, and G. Manimaran, "Vulnerability assessment of cybersecurity for scada systems," *IEEE Transactions on Power Systems*, vol. 23, no. 4, pp. 1836–1846, 2008.

[16] H. Bevrani, *Robust power system frequency control*. Springer, 2014.

[17] L. L. Grigsby, *Power system stability and control*. CRC press, 2012, vol. 5.

[18] M. S. Mahmoud, M. M. Hamdan, and U. A. Baroudi, "Modeling and control of cyber-physical systems subject to cyber attacks: A survey of recent advances and challenges," *Neurocomputing*, vol. 338, pp. 101–115, 2019.

[19] M. S. Mahmoud and Y. Xia, *Cloud Control Systems: Analysis, Design and Estimation*. Academic Press, 2020.

[20] B. S. Rithigaa, K. Vamshi, A. Jawahar, and K. Ramakrishnan, "Lyapunov stability analysis of load frequency control systems with communication network induced time-delays and ev aggregator," in *2021 9th IEEE International Conference on Power Systems (ICPS)*. IEEE, 2021, pp. 1–6.

[21] A. Jawahar and K. Ramakrishnan, "Further improvement in stability and stabilization margin of micro-grid load frequency control system with constant communication delays," in *Proceedings of Symposium on Power Electronic and Renewable Energy Systems Control*. Springer, 2021, pp. 185–194.

[22] A. Dev, V. Léchappé, and M. K. Sarkar, "Prediction-based super twisting sliding mode load frequency control for multi-area interconnected power systems with state and input time delays using disturbance observer," *International Journal of Control*, vol. 94, no. 7, pp. 1751–1764, 2021.

[23] M. S. Mahmoud and Y. Xia, *Networked control systems: cloud control and secure control*. Butterworth-Heinemann, 2019.

[24] Z. Song, Y. Liu, and M. Tan, "Robust pinning synchronization of complex cyberphysical networks under mixed attack strategies," *International Journal of Robust and Nonlinear Control*, vol. 29, no. 5, pp. 1265–1278, 2019.

[25] C.-H. Xie and G.-H. Yang, "Observer-based attack-resilient control for linear systems against fdi attacks on communication links from controller to actuators," *International Journal of Robust and Nonlinear Control*, vol. 28, no. 15, pp. 4382–4403, 2018.

[26] S. Sridhar and G. Manimaran, "Data integrity attacks and their impacts on scada control system," in *IEEE PES general meeting*. IEEE, 2010, pp. 1–6.

[27] S. Liu, X. P. Liu, and A. El Saddik, "Denial-of-service (dos) attacks on load frequency control in smart grids," in *2013 IEEE PES Innovative Smart Grid Technologies Conference (ISGT)*. IEEE, 2013, pp. 1–6.

[28] K. Rahimi, A. Parchure, V. Centeno, and R. Broadwater, "Effect of communication time-delay attacks on the performance of automatic generation control," in *2015 North American Power Symposium (NAPS)*. IEEE, 2015, pp. 1–6.

[29] J. Zhang and A. D. Domínguez-García, "On the impact of communication delays on power system automatic generation control performance," in *2014 North American Power Symposium (NAPS)*. IEEE, 2014, pp. 1–6.

[30] H. Bevrani and T. Hiyama, "On load–frequency regulation with time delays: design and real-time implementation," *IEEE transactions on energy conversion*, vol. 24, no. 1, pp. 292–300, 2009.

[31] L. Jiang, W. Yao, Q. Wu, J. Wen, and S. Cheng, "Delay-dependent stability for load frequency control with constant and time-varying delays," *IEEE Transactions on Power systems*, vol. 27, no. 2, pp. 932–941, 2011.

[32] S. Liu, P. X. Liu, and A. El Saddik, "Modeling and stability analysis of automatic generation control over cognitive radio networks in smart grids," *IEEE Transactions on Systems, Man, and Cybernetics: Systems*, vol. 45, no. 2, pp. 223–234, 2014.

[33] W. Tan, "Tuning of pid load frequency controller for power systems," *Energy Conversion and Management*, vol. 50, no. 6, pp. 1465–1472, 2009.

[34] C.-T. Pan and C.-M. Liaw, "An adaptive controller for power system load-frequency control," *IEEE Transactions on Power Systems*, vol. 4, no. 1, pp. 122–128, 1989.

[35] Z.-Q. Wang and M. Sznaier, "Robust control design for load frequency control using/spl mu/-synthesis," in *Conference Record Southcon*. IEEE, 1994, pp. 186–190.

[36] G. Ray, A. Prasad, and G. Prasad, "A new approach to the design of robust load-frequency controller for large scale power systems," *Electric power systems research*, vol. 51, no. 1, pp. 13–22, 1999.

[37] H. M. Soliman, A. Dabroum, M. S. Mahmoud, and M. Soliman, "Guaranteed-cost reliable control with regional pole placement of a power system," *Journal of the Franklin Institute*, vol. 348, no. 5, pp. 884–898, 2011.

[38] C. Chang and W. Fu, "Area load frequency control using fuzzy gain scheduling of pi controllers," *Electric Power Systems Research*, vol. 42, no. 2, pp. 145–152, 1997.

[39] J. Talaq and F. Al-Basri, "Adaptive fuzzy gain scheduling for load frequency control," *IEEE Transactions on power systems*, vol. 14, no. 1, pp. 145–150, 1999.

[40] D. Wang, F. Chen, B. Meng, X. Hu, and J. Wang, "Event-based secure h∞ load frequency control for delayed power systems subject to deception attacks," *Applied Mathematics and Computation*, vol. 394, p. 125788, 2021.

[41] D. Rerkpreedapong, A. Hasanovic, and A. Feliachi, "Robust load frequency control using genetic algorithms and linear matrix inequalities," *IEEE Transactions on Power Systems*, vol. 18, no. 2, pp. 855–861, 2003.

[42] X. Yu and K. Tomsovic, "Application of linear matrix inequalities for load frequency control with communication delays," *IEEE transactions on power systems*, vol. 19, no. 3, pp. 1508–1515, 2004.

[43] I. Furtat, A. Nekhoroshikh, and P. Gushchin, "Synchronization of multi-machine power systems under disturbances and measurement errors," *International Journal of Adaptive Control and Signal Processing*, 2022.

[44] Y. S. Qudaih, M. Bernard, Y. Mitani, and T. Mohamed, "Model predictive based load frequency control design in the presence of dfig wind turbine," in *2011 2nd International Conference on Electric Power and Energy Conversion Systems (EPECS)*. IEEE, 2011, pp. 1–5.

[45] F. Kamal and B. Chowdhury, "Model predictive control and optimization of networked microgrids," *International Journal of Electrical Power & Energy Systems*, vol. 138, p. 107804, 2022.

[46] A. Oshnoei, M. Kheradmandi, S. Muyeen, and N. D. Hatziargyriou, "Disturbance observer and tube-based model predictive controlled electric vehicles for frequency regulation of an isolated power grid," *IEEE Transactions on Smart Grid*, vol. 12, no. 5, pp. 4351–4362, 2021.

[47] R. Sedaghati and M. R. Shakarami, "Power sharing adaptive control strategy for a microgrid with multiple storage and renewable energy sources," *International Journal of Adaptive Control and Signal Processing*, vol. 32, no. 11, pp. 1607–1628, 2018.

[48] L.-R. Chang-Chien, Y.-S. Wu, and J.-S. Cheng, "Online estimation of system parameters for artificial intelligence applications to load frequency control," *IET generation, transmission & distribution*, vol. 5, no. 8, pp. 895–902, 2011.

[49] M. Rahmani and N. Sadati, "Hierarchical optimal robust load-frequency control for power systems," *IET generation, transmission & distribution*, vol. 6, no. 4, pp. 303–312, 2012.

[50] M. S. Mahmoud and O. Al-Buraiki, "Two-level control for improving the performance of microgrid in islanded mode," in *2014 IEEE 23rd International Symposium on Industrial Electronics (ISIE)*. IEEE, 2014, pp. 254–259.

[51] F. Daneshfar, "Intelligent load-frequency control in a deregulated environment: continuous-valued input, extended classifier system approach," *IET generation, transmission & distribution*, vol. 7, no. 6, pp. 551–559, 2013.

[52] A. Rahman, L. C. Saikia, and N. Sinha, "Load frequency control of a hydro-thermal system under deregulated environment using biogeography-based optimised three-degree-of-freedom integral-derivative controller," *IET generation, transmission & distribution*, vol. 9, no. 15, pp. 2284–2293, 2015.

[53] Y. Mi, X. Hao, Y. Liu, Y. Fu, C. Wang, P. Wang, and P. C. Loh, "Sliding mode load frequency control for multi-area time-delay power system with wind power integration," *IET Generation, Transmission & Distribution*, vol. 11, no. 18, pp. 4644–4653, 2017.

[54] C. Fu and W. Tan, "Decentralised load frequency control for power systems with communication delays via active disturbance rejection," *IET Generation, Transmission & Distribution*, vol. 12, no. 6, pp. 1397–1403, 2017.

[55] W. T. Miller, P. J. Werbos, and R. S. Sutton, *Neural networks for control*. MIT press, 1995.

[56] P. J. Werbos, T. McAvoy, and T. Su, "Handbook of intelligent control," *chap. neurocontrol and supervised learning: An overview and evaluation. New York: Van Nostrand Rheinhold*, 1992.

[57] R. S. Sutton and A. G. Barto, *Reinforcement learning: An introduction*. MIT press, 2018.

[58] F. L. Lewis, D. Vrabie, and V. L. Syrmos, *Optimal control*. John Wiley & Sons, 2012.

[59] A. E. Bryson, "Optimal control-1950 to 1985," *IEEE Control Systems Magazine*, vol. 16, no. 3, pp. 26–33, 1996.

[60] J. Li, T. Yu, and X. Zhang, "Coordinated load frequency control of multi-area integrated energy system using multi-agent deep reinforcement learning," *Applied Energy*, vol. 306, p. 117900, 2022.

[61] S. SEN, "Learning in multiagent systems [in:] weiss g., ed., multiagentsystems: A modern approach to distributed artificial intelligence, chapitre 6," 1999.

[62] N. M. Alyazidi, M. S. Mahmoud, and M. I. Abouheaf, "Adaptive critics based cooperative control scheme for islanded microgrids," *Neurocomputing*, vol. 272, pp. 532–541, 2018.

[63] M. S. Mahmoud, N. M. Alyazidi, and M. I. Abouheaf, "Adaptive intelligent techniques for microgrid control systems: A survey," *International Journal of Electrical Power & Energy Systems*, vol. 90, pp. 292–305, 2017.

[64] Q. Su, W. Quan, G. Cai, and J. Li, "An improved adaptive backstepping approach on static var compensator controller of nonlinear power systems," *International Journal of Adaptive Control and Signal Processing*, vol. 32, no. 5, pp. 700–712, 2018.

[65] A. Gundes and L. Kabuli, "Load frequency control of multi-area interconnected power systems with time delays," *IEEE Transactions on Control of Network Systems*, 2021.

[66] S. Feng, P. Tesi, and C. De Persis, "Towards stabilization of distributed systems under denial-of-service," in *2017 IEEE 56th Annual Conference on Decision and Control (CDC)*. IEEE, 2017, pp. 5360–5365.

[67] C. De Persis, R. Sailer, and F. Wirth, "On inter-sampling times for event-triggered large-scale linear systems," in *52nd IEEE Conference on Decision and Control*. IEEE, 2013, pp. 5301–5306.

[68] M. Mazo and P. Tabuada, "Decentralized event-triggered control over wireless sensor/actuator networks," *IEEE Transactions on Automatic Control*, vol. 56, no. 10, pp. 2456–2461, 2011.

[69] M. S. Mahmoud and H. N. Nounou, "Simultaneous output feedback stabilization of time-delay systems," *IMA Journal of Mathematical Control and Information*, vol. 23, no. 2, pp. 211–223, 2006.

[70] S. Dashkovskiy, H. Ito, and F. Wirth, "On a small gain theorem for iss networks in dissipative lyapunov form," *European Journal of Control*, vol. 17, no. 4, pp. 357–365, 2011.

[71] A. Molina-García, I. Munoz-Benavente, A. D. Hansen, and E. Gomez-Lazaro, "Demand-side contribution to primary frequency control with wind farm auxiliary control," *IEEE transactions on power systems*, vol. 29, no. 5, pp. 2391–2399, 2014.

[72] M. S. Mahmoud and M. M. Hamdan, "Stabilization of distributed cyber physical systems subject to denial-of-service attack," *International Journal of Control*, pp. 1–11, 2020.

[73] C. De Persis and P. Tesi, "Input-to-state stabilizing control under denial-of-service," *IEEE Transactions on Automatic Control*, vol. 60, no. 11, pp. 2930–2944, 2015.

[74] H. Saadat *et al.*, *Power system analysis*. McGraw-hill, 1999, vol. 2.

[75] K. Pan, J. Dong, E. Rakhshani, and P. Palensky, "Effects of cyber attacks on ac and high-voltage dc interconnected power systems with emulated inertia," *Energies*, vol. 13, no. 21, p. 5583, 2020.

[76] M. Abouheaf, F. Lewis, S. Haesaert, R. Babuska, and K. Vamvoudakis, "Multi-agent discrete-time graphical games: interactive nash equilibrium and value it-

eration solution," in *2013 American Control Conference*. IEEE, 2013, pp. 4189–4195.

[77] B. Widrow, N. K. Gupta, and S. Maitra, "Punish/reward: Learning with a critic in adaptive threshold systems," *IEEE Transactions on Systems, Man, and Cybernetics*, no. 5, pp. 455–465, 1973.

[78] M. M. Hamdan, M. S. Mahmoud, and Y. Xia, "Coordination control strategies for multivehicle systems," *Journal of the Franklin Institute*, vol. 357, no. 17, pp. 12 197–12 222, 2020.

[79] S. Riverso, M. Farina, and G. Ferrari-Trecate, "Plug-and-play state estimation and application to distributed output-feedback model predictive control," *European journal of Control*, vol. 25, pp. 17–26, 2015.

[80] M. Abouheaf and W. Gueaieb, "Online model-free controller for flexible wing aircraft: a policy iteration-based reinforcement learning approach," *International Journal of Intelligent Robotics and Applications*, pp. 1–23, 2019.

[81] M. Ma, H. Chen, X. Liu, and F. Allgöwer, "Distributed model predictive load frequency control of multi-area interconnected power system," *International Journal of Electrical Power & Energy Systems*, vol. 62, pp. 289–298, 2014.

VITAE

- Name: Yousif Ahmed Saeed Ghaleb Al-Wajih
- Nationality: Yemen
- Date of Birth: 01/01/1994
- Email: *alwajihyousif@gmail.com*
- Permanent Address: Taiz 96704, Yemen

Education

2015-2020	B.Sc Control and instrumentation System Engineering King Fahd University of Petroleum and Minerals, Saudi Arabia.
2020-present	M.Sc Systems and Control Engineering King Fahd University of Petroleum and Minerals, Saudi Arabia.

Publications Under Review

- N.M. Al-Yazidi, Y.A. Al-Wajih, and M.S. Mahmoud, "Iterative Adaptive Control Design for Multi-Area Power System," *International Journal of Adaptive Control and Signal Processing*, (2022).

- Y.A. Al-Wajih, N.M. Al-Yazidi, Hamdan M.H., and M.S. Mahmoud, "Stability Analysis of Multi-area Interconnected Power System Under Transmission Delay," *International Journal of Control*, (2022).

- Hamdan M.H., Y.A. Al-Wajih, and M.S. Mahmoud, "Stability Analysis of Multi-area Interconnected Power System Subject to Denial of Service Attack," *International Journal of Systems Science*, (2021).